Inorg. Chem. **2008**, *47*, 8896−8911

Synthesis, Structure and Magnetic Behavior of Five-Coordinate Bis(iminopyrrolyl) Complexes of Cobalt(II) containing PMe_3 and THF Ligands

Sónia A. Carabineiro,[†] Ronan M. Bellabarba,[†] Pedro T. Gomes,[*,†] Sofia I. Pascu,[‡] Luís F. Veiros,[†] Cristina Freire,[§] Laura C. J. Pereira,[||] Rui T. Henriques,[¶] M. Conceição Oliveira,[†] and John E. Warren[¥]

Centro de Química Estrutural, Departamento de Engenharia Química e Biológica, Instituto Superior Técnico, Avenida Rovisco Pais, 1049-001 Lisboa, Portugal, Department of Chemistry, University of Bath, Bath BA2 7AY, United Kingdom; REQUIMTE/Departamento de Química, Faculdade de Ciências, Universidade do Porto, Rua Campo Alegre, 4169-007 Porto, Portugal, Departamento de Química, Instituto Tecnológico e Nuclear/CFMCUL, Estrada Nacional 10, 2686-953 Sacavém, Portugal, Instituto de Telecomunicações, Instituto Superior Técnico, Avenida Rovisco Pais, 1049-001 Lisboa, Portugal, and Science & Technology Facilities Council Daresbury Laboratory, Warrington, Cheshire, WA4 4AD, United Kingdom

Received May 30, 2008

The new bis-iminopyrrolyl five-coordinate Co(II) complexes [Co(κ^2*N*,*N*′-NC_4H_3C(R)═N-2,6-$^i Pr_2C_6H_3$)$_2$(PMe_3)] (R = H **3a**; Me **3b**) were synthesized in high yields (ca. 80−90%), using THF and diethyl ether as solvents, respectively, by (a) treatment of $CoCl_2(PMe_3)_2$ with the corresponding iminopyrrolyl Na salts (**Ie** or **If**) or (b) reaction of anhydrous $CoCl_2$ and PMe_3 with **Ie** or **If**. A third route was tested, involving the addition of excesses of PMe_3 to the complexes [Co(κ^2*N*,*N*′-NC_4H_3C(R)═N-2,6-$^i Pr_2C_6H_3$)$_2$] (R = H **1e**; Me **1f**), which was only successful for the synthesis of **3a**, in lower yields (ca. 30%). The synthesis of **3b** in THF was unfruitful because of the kinetic competition of the solvent, giving rise to mixtures of **1f** and its coordinated THF adduct **4b**. The synthesis of the new bis-iminopyrrolyl five-coordinate Co(II) complexes [Co(κ^2*N*,*N*′-NC_4H_3C(R)═N-2,6-$^i Pr_2C_6H_3$)$_2$(THF)] (R = H **4a**; Me **4b**) were carried out in high yields (ca. 80−90%) by the reaction of $CoCl_2(THF)_{1.5}$ with the corresponding iminopyrrolyl Na salt. All the compounds have been characterized by X-ray diffraction, with **3a** and **3b** showing axially compressed trigonal bipyramidal geometry (with the PMe_3 ligand lying on the equatorial plane), whereas complexes **4a** and **4b** exhibit distorted square pyramidal geometries with the THF molecule occupying the axial position. Complex **4a** shows clearly a compressed geometry, but for complex **4b**, two polymorphs were characterized, exhibiting molecules with different Co−O (THF) bond lengths, one of them being compatible with an elongated form. Magnetic measurements either in the solid or in the liquid phases indicate that complexes **3a** and **3b** have low-spin ground states ($S = 1/2$). In toluene solution, the geometry is fully confirmed by EPR data, which further indicates a $d_{x^2-y^2}/d_{xy}$ ground state. However, compounds **4a** and **4b** behave unusually because they show magnetic moments that are compatible with high-spin ground states ($S = 3/2$) in the solid state, but conform to low-spin ground states ($S = 1/2$) when both complexes are dissolved in toluene solutions. The low-spin ground states in toluene solution are confirmed by EPR spectroscopy, which further supports, for complexes **4a** and **4b**, an axially elongated square pyramidal geometry and a d_{z^2} ground state. Thus the change in the ground-state and, consequently, in the geometry of complexes **4a** and **4b** from solid state to toluene solution might be a consequence of the elongation of the Co−O(THF) bond length. DFT studies performed on complexes **3** and **4** corroborate their different structure and magnetic behaviors and verify, for the latter complexes, the structural differences observed in the solid state and in toluene solution.

Introduction

Schiff base-derived ligands have been widely used as efficient frameworks for the preparation of metal complexes with various applications in research fields, such as materials science or homogeneous catalysis. However, metal complexes of bidentate ligands containing both an imine and a pyrrolyl moiety are still scarce. Despite 2-iminopyrrolyl

* To whom correspondence should be addressed. E-mail: pedro.t.gomes@ist.utl.pt. Phone: +351 218419612. Fax: +351 218419612.
[†] Instituto Superior Técnico (CQE).
[‡] University of Bath.
[§] University of Porto.
[||] Instituto Tecnológico e Nuclear/CFMCUL.
[¶] Instituto Superior Técnico (IT).
[¥] Daresbury Laboratory.

10.1021/ic800992f CCC: $40.75
Published on Web 08/20/2008

Chart 1

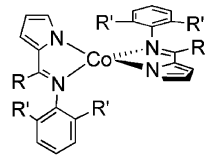

1a R = R'= H, **1d** R = R' = Me
1b R = Me, R'= H **1e** R = H, R' = ^{i}Pr
1c R = H, R' = Me

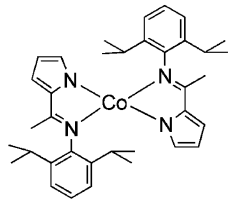

1f

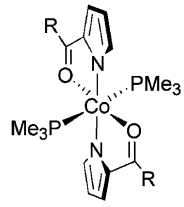

2a R = H,
2b R = Me

ligands having been used for a long time,[1] interest in them has increased only more recently when employed as building blocks of α-olefin polymerization metal catalysts.[2−4] In view of the fact that bulky aryl substituents in the imine group provide steric tuning and shielding of the metal centers, leading to modified reactivities and increased stability of the catalytic species, several mono- or bis(2-iminopyrrolyl) early and, to a smaller extent, late transition-metal complexes have been reported in the literature, which are efficient α-olefin oligo/polymerization catalysts.[2] These bulky ligands have also been used in the synthesis of homoleptic transition-metal complexes of the type [M(2-iminopyrrolyl)$_2$] (M= Co,[5,6] Ni,[5,7] Zn[8]).

In a previous work, we have synthesized and characterized a series of four-coordinate Co(II) bis-iminopyrrolyl complexes [Co(κ^2-*N*,*N*′-NC$_4$H$_3$C(R)=N-2,6-R′$_2$C$_6$H$_3$)$_2$],[6] most of them showing a high-spin (S = 3/2) tetrahedral geometry (Chart 1, **1a**−**e**). However, when a combination of high stereochemical interligand repulsion and electronic donation of the imino group was employed, such as in the case of R = Me and R′ = ^{i}Pr, the complex structure switched to a low-spin (S = 1/2) square planar geometry (Chart 1, **1f**).

Recently, we have also reported on the preparation and characterization of Co(II) complexes containing bidentate N,O 2-formyl- and 2-acetylpyrrolyl ligands (Chart 1, **2a**, **b**).[9] The ketopyrrolyl ligands used in that work are the parent compounds of the 2-iminopyrrolyl ligands referred above and are simultaneously less sterically demanding and weaker electronic donors than their corresponding isoelectronic N,N counterparts. Therefore, species analogous to **1** ([Co(κ^2-*N*,*O*-2-ketopyrrolyl)$_2$]) are not stable and can only be isolated when stabilized by neutral donor ligands such as PMe$_3$, affording six-coordinate octahedral 19-electron complexes in which the Co(II) center is in a low-spin ground state (d_{z^2}, S = 1/2).[9]

Similarly, complexes **1**, although existing as stable entities, are unsaturated (formally 15-electron compounds) and are sensitive to small neutral donor molecules such as O$_2$ or H$_2$O. In the present work, we describe the preparation and characterizations of PMe$_3$ and THF adducts of **1e** and **1f**, using different chemical routes. The compounds obtained were fully characterized by several techniques such as elemental analysis, X-ray diffraction, magnetic susceptibility measurements, EPR spectroscopy, and DFT calculations. They showed structures varying from the unusual axially compressed trigonal bipyramidal (TBP) to distorted square pyramidal (SP) geometries and different magnetic properties. In fact, the magnetic behavior of cobalt(II) complexes, in particular that of five-coordinate complexes, is not straightforward and dramatic changes may occur because of subtle distortions in their geometries.[10]

Results and Discussion

Synthesis of Complexes. The reaction of a solution of CoCl$_2$(PMe$_3$)$_2$, in THF, with 2 equiv of the bidentate ligand precursor **Ie**, obtained by in situ deprotonation of the corresponding 2-formiminopyrrole with NaH,[6,7] and further extraction of the reaction products in *n*-hexane, afforded an almost quantitative amount of the five-coordinate complex [Co(κ^2*N*,*N*′-NC$_4$H$_3$C(H)=N-2,6-^{i}Pr$_2$C$_6$H$_3$)$_2$(PMe$_3$)] (**3a**) (Scheme 1, route a). This compound can be formulated as a 17-electron species and was obtained as a dark red crystalline paramagnetic material, its solutions being particularly sensitive to air. The corresponding molecular structure was confirmed by X-ray diffraction and EPR spectroscopy (see below). Unlike the reaction of CoCl$_2$(PMe$_3$)$_2$ with 2-ketopyrrolyl sodium salts, where octahedral complexes of [Co(κ^2*N*,*O*-NC$_4$H$_3$C(R)=O)$_2$(PMe$_3$)$_2$] (R = H, Me) were obtained,[9] a PMe$_3$

(1) Holm, R. H.; Chakravorty, A.; Theriot, L. J. *Inorg. Chem.* **1966**, *5*, 625–635, and references cited therein.
(2) Mashima, K.; Tsurugi, H. *J. Organomet. Chem.* **2005**, *690*, 4414–4423, and references cited therein.
(3) Britovsek, G; J, P.; Gibson, V. C.; Wass, D. F. *Angew. Chem., Int. Ed.* **1999**, *38*, 428–447, and references cited therein.
(4) Gibson, V. C.; Spitzmesser, S. K. *Chem. Rev.* **2003**, *103*, 283–315, and references cited therein.
(5) Dawson, D. M.; Walker, D. A.; Thornton-Pett, M.; Bochmann, M. *J. Chem. Soc., Dalton Trans.* **2000**, 459–466.
(6) Carabineiro, S. A.; Silva, L. C.; Gomes, P. T.; Pereira, L. C. J.; Veiros, L. F.; Pascu, S. I.; Duarte, M. T.; Namorado, S.; Henriques, R. T. *Inorg. Chem.* **2007**, *46*, 6880–6890.
(7) Bellabarba, R. M.; Gomes, P. T.; Pascu, S. I. *Dalton Trans.* **2003**, 4431–4436.
(8) Hao, H.; Bhandari, S.; Ding, Y.; Roesky, H. W.; Magull, J.; Schmidt, H. G.; Noltemeyer, M.; Cui, C. *Eur. J. Inorg. Chem.* **2002**, 1060–1065.
(9) Carabineiro, S. A.; Gomes, P. T.; Veiros, L. F.; Freire, C.; Pereira, L. C. J.; Henriques, R. T.; Warren, J. E.; Pascu, S. I. *Dalton Trans.* **2007**, 5460–5470.
(10) For instance, see: (a) Berry, J. F.; Cotton, F. A.; Liu, C. Y.; Lu, T.; Murillo, C. A.; Tsukerblat, B. S.; Villagrán, D.; Wang, X. *J. Am. Chem. Soc.* **2005**, *127*, 4895–4902, and references cited therein. (b) Galet, A.; Gaspar, A. B.; Muñoz, M. C.; Real, J. A. *Inorg. Chem.* **2006**, *45*, 4413–4422. (c) Cotton, F. A.; Wilkinson, G.; Murillo, C. A.; Bochmann, M. *Advanced Inorganic Chemistry*, 6th ed.; John Wiley & Sons: New York, 1999; p. 822.

Scheme 1. Syntheses of Complex **3a** in THF

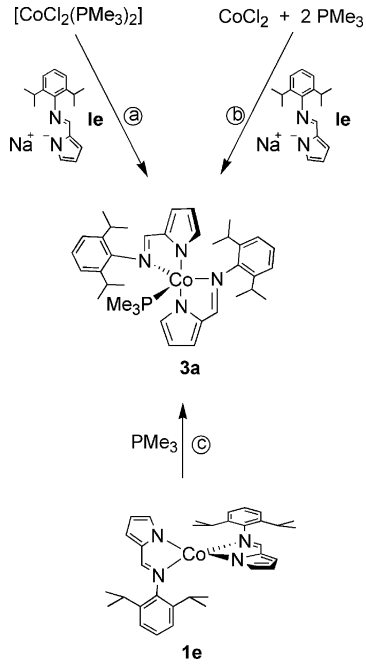

Scheme 2. Syntheses of Complex **3b** in Et_2O

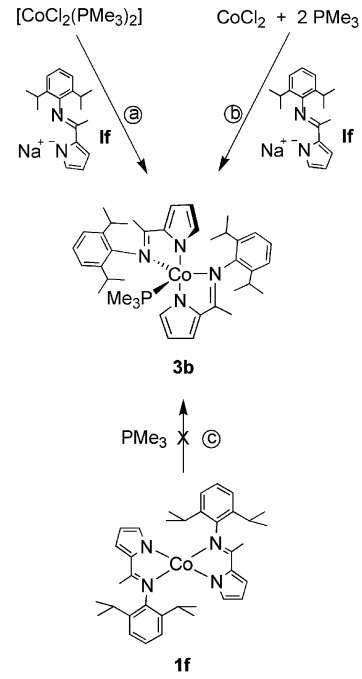

ligand was expelled from the Co(II) coordination sphere, giving rise to a distorted trigonal bipyramidal (TBP) geometry (see below). This is a consequence of the bulkiness of the 2,6-diisopropylphenyl substituents of the iminic nitrogens. If a stoichiometric amount of ligand precursor is used, the same compound is obtained with 40% yield and not the expected monosubstituted [Co(κ^2N,N'-$NC_4H_3C(H)$=N-2,6-$^{i}Pr_2C_6H_3)_2(PMe_3)_{2-n}Cl$] ($n$ = 0 or 1) species.

Following the syntheses of **3a**, we prepared the analogous dark red paramagnetic compound [Co(κ^2N,N'-NC_4H_3C(Me)=N-2,6-$^{i}Pr_2C_6H_3)_2(PMe_3)$] (**3b**), containing a methyl substituent on the iminic carbon, using exactly the same methodologies (Scheme 2), but using Et_2O as solvent. Indeed, in both synthetic routes a and b, high yields (87% and 86%, respectively) of complex **3b** were obtained. Its molecular structure was determined by X-ray diffraction, EPR spectroscopy, and ESI-MS (see below). However, attempts to synthesize compound **3b** by route c, in Et_2O, did not succeed using excess amounts (1:5) of PMe_3 and reaction times up to 7 days, highlighting the stereochemically hindered nature of complex **1f**.

The same synthetic procedures for the preparation of **3b** were also attempted in THF. In fact, the reaction of $CoCl_2(PMe_3)_2$ with 2 equiv of the sodium salt **If** (Scheme 3, route a) gave, after 2 h of reaction, a first crop of crystals (39%) of the desired compound **3b**. However, a second crop (55%) of square planar complex **1f**[6] was also obtained, which was characterized by elemental analysis and EPR (see below). When the same reaction was carried out for 12 h, a second crop of **1f** was similarly obtained, but this time compound **3b** was not present in the first crop. In fact, the latter contained more than a single species, which could not be clearly identified either by EPR spectroscopy or elemental analyses. However, ESI-MS experiments showed the absence of **3b**, and the presence of the square planar complex **1f** and a different complex [Co(κ^2N,N'-NC_4H_3C(Me)=N-2,6-$^{i}Pr_2C_6H_3)_2$(THF)] (**4b**), where a molecule of the solvent was coordinated to the Co(κ^2N,N'-NC_4H_3C(Me)=N-2,6-$^{i}Pr_2C_6H_3)_2$ fragment, instead of a PMe_3 ligand. Some single crystals could also be isolated from the bulk product, their X-ray diffraction analysis confirming the molecular structure of compound **4b** (polymorph **4b_II**, see X-ray diffraction). The formation of **1f** and **4b** possibly results from the kinetic instability of **3b** in the THF reaction mixture, leading to the replacement of PMe_3 by the solvent. Alternatively, they can arise from the presence of $[CoCl_2(THF)_x(PMe_3)_{2-x}]$ species likely originated, either by coordination to or exchange of solvent molecules with the starting reagent $CoCl_2(PMe_3)_2$. The weaker donor capacity and lower steric influence of the THF ligand in complex **4b** (cone angles (equivalent) of 106° and 88°, respectively, taken along and perpendicularly to the C−O−C plane of THF[11]), in comparison with PMe_3 (cone angle (equivalent) = 111°[11]), together with a higher steric hindrance and electron donation of the **If** ligand framework, in comparison with **Ie**,[6] may facilitate the release of the THF molecule from the Co coordination sphere, giving rise to the square planar complex **1f**. In fact, the formation of the formimino analogue of **4b** (**4a**, see below) was not observed in the preparation of **3a** in THF.

The reaction of the sodium salt **If** with a mixture of anhydrous $CoCl_2$ and 2 equiv of PMe_3 (Scheme 3, route b), in THF, for 2 or 12 h, gave the square planar complex **1f** as the only product obtained. No traces of **3b** or **4b** could be detected. In fact, the anhydrous $CoCl_2$, virtually insoluble in THF, reacts faster with the sodium salt **If** than with PMe_3. The nonformation of **3b** or **4b** is a consequence of the high

(11) Marçalo, J. Private communication. The cone angle (equivalent) values were calculated on the basis of solid angles measurements according to Marçalo, J.; de Matos, A. P. *Polyhedron* **1989**, *8*, 2431–2437. For cone angle definition and calculation, see, for example: (a) Tolman, C. A. *Chem. Rev.* **1977**, *77*, 313–348. (b) Dias, P. B.; da Piedade, M. E. M.; Simões, J. A. M. *Coord. Chem. Rev.* **1994**, *135*, 737–807.

Scheme 3. Synthesis Attempts of Complex **3b** in THF

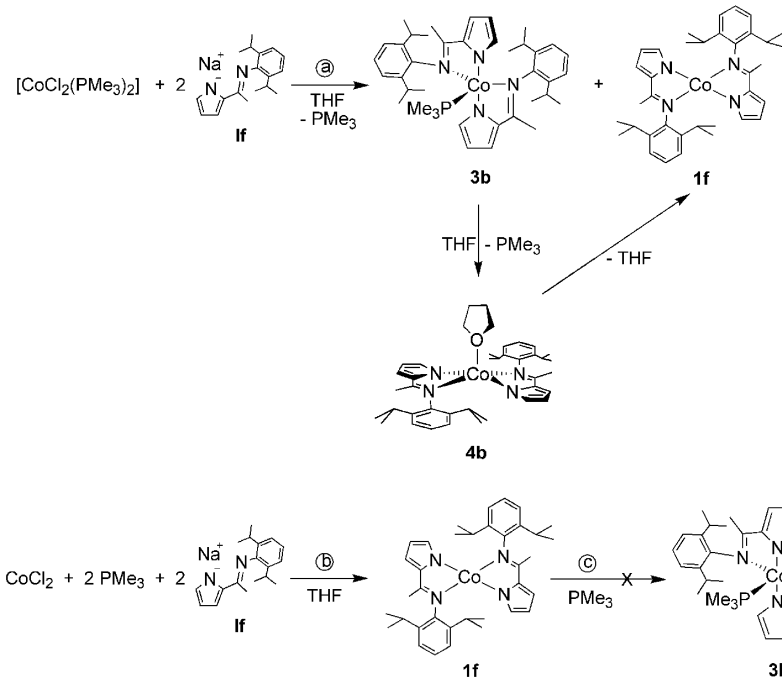

Scheme 4. Syntheses of Complexes **4a** and **4b** in THF

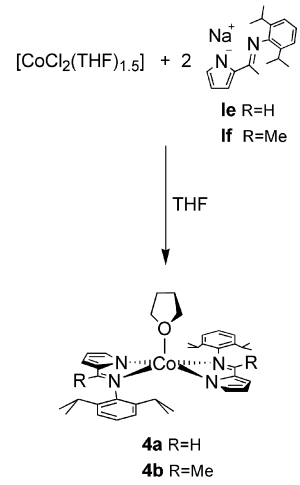

stereochemical hindrance observed in that square planar complex because of the presence of the methyl substituents of the iminic carbons[6] that subsequently prevent the coordination of either the PMe_3 ligand or the THF solvent molecules to **1f**. For the same reasons, several attempts to prepare compound **3b** by addition of an excess of PMe_3 to **1f** (Scheme 3, route c), in THF, varying the temperature (room temperature and 50 °C) and reaction time (up to 5 days, at both temperatures), were unfruitful. This behavior shows a marked difference in the reactivities of **1e** and **1f** toward PMe_3 and THF ligands.

As in the case of **3a**, the attempts to prepare **3b** starting from $CoCl(PMe_3)_3$ (instead of $[CoCl_2(PMe_3)_2]$), in THF, were unsuccessful.

To isolate complex **4b** in a pure state and perform its full characterization, we have used $[Co_4Cl_8(THF)_6]$ $(CoCl_2(THF)_{1.5})$[12] as starting material, as shown in Scheme 4. Compound **4b**, as well as its formimino analogue $[Co(\kappa^2N,N'\text{-}NC_4H_3C(H)=N\text{-}2,6\text{-}{}^iPr_2C_6H_3)_2(OC_4H_8)]$ (**4a**), were obtained in high yields (84 and 92%, respectively), as paramagnetic dark red crystals, that were characterized by elemental analysis, X-ray diffraction, magnetic susceptibility measurements, and EPR spectroscopy. Another crystalline polymorph of **4b** (**4b_I**) was obtained in the crystallization of this reaction product (see X-ray diffraction).

X-ray Diffraction. Crystals suitable for X-ray diffraction were obtained for all compounds, **3a**, **3b**, **4a**, and **4b**, enabling the determination of their crystal and molecular structures (two polymorphs of the latter compound were measured: **4b_I** and **4b_II**). Selected bond distances (Å) and angles (°) are listed in Table 1.

The molecular structure of complex **3a** is shown in Figure 1a.[13] This Co(II) complex has an unusual coordination geometry around the cobalt atom, generated by N1−N2−N3−N4-P1 atoms, which can be described as axially compressed trigonal bipyramidal. In fact, the axial positions are occupied by the anionic pyrrolyl rings of both bidentate ligands, which are trans to each other, with an almost linear N3−Co1−N1 axis (176.35(7)°), being Co1−N1 and Co1−N3 (1.9153(16)

(12) (a) Kern, R. J. *J. Inorg. Nucl. Chem.* **1962**, *24*, 1105–1109. (b) Fowles, G. W. A.; Rice, D. A.; Walton, R. A. *J. Inorg. Nucl. Chem.* **1969**, *31*, 3119–3131. (c) Sobota, P.; Olejnik, Z.; Utko, J.; Lis, T. *Polyhedron* **1993**, *12*, 613–616.

(13) In the first attempt to synthesise **3a** by route b (Scheme 1), almost certainly carried out in sub-optimal experimental conditions, a material was isolated with CHN elemental analysis values higher than expected. X-ray diffraction showed a crystal structure containing **3a** co-crystallized with the neutral acetiminopyrrole ligand precursor in a ratio of 1:1 (**3a·L**). The molecular features of the Co complex of **3a·L** are very similar to those of **3a** (see Table S1 and Figures S2 and S3 of Supporting Information).

Table 1. Selected Bond Distances (Å) and Angles (deg) for Compounds **3a**, **3b**, **4a**, and **4b** (Polymorphs **4b_I** and **4b_II**)

	3a	3b	4a	4b_I	4b_II
Co(1)−P(1)	2.2580(5)	2.2387(15)			
Co(1)−O(1)			2.0484(17)	2.103(2)	2.182(12)
Co(1)−N(1)	1.9153(16)	1.903(2)	2.0820(18)	2.014(2)	2.055(4)
Co(1)−N(2)	2.0483(16)	2.059(2)	2.0899(17)	2.112(2)	2.073(4)
Co(1)−N(3)	1.9214(16)		2.0814(18)	2.020(2)	
Co(1)−N(4)	2.0481(16)		2.0942(17)	2.110(2)	
P(1)−C(39)	1.824(2)	1.835(5)			
P(1)−C(38)	1.820(2)	1.787(4)			
P(1)−C(37)	1.821(2)	1.803(4)			
N(1)−C(4)	1.382(2)	1.377(4)	1.371(3)	1.381(3)	1.375(6)
N(1)−C(1)	1.351(3)	1.357(4)	1.353(3)	1.354(3)	1.359(6)
N(2)−C(5)	1.307(2)	1.305(4)	1.298(3)	1.299(3)	1.294(6)
N(2)−C(13)	1.434(2)	1.432(4)	1.429(2)	1.431(3)	1.438(6)
N(4)−C(11)	1.304(3)		1.295(3)	1.302(3)	
N(4)−C(19)	1.434(3)		1.435(3)	1.437(3)	
N(3)−C(10)	1.385(3)		1.370(3)	1.381(3)	
N(3)−C(7)	1.348(3)		1.348(3)	1.350(3)	
P(1)−Co(1)−N(1)	93.78(5)	91.69(9)			
P(1)−Co(1)−N(2)	112.47(5)	107.81(8)			
P(1)−Co(1)−N(4)	106.27(5)				
P(1)−Co(1)−N(3)	89.90(5)				
O(1)−Co(1)−N(1)				97.02(8)	94.40(9)
O(1)−Co(1)−N(2)				105.04(8)	100.56(8)
N(1)−Co(1)−N(4)	96.81(7)		95.10(7)	98.53(8)	
N(2)−Co(1)−N(4)	141.24(7)		145.64(6)	160.45(8)	
N(2)−Co(1)−N(2_1)		144.38(15)			144.2(2)
N(1)−Co(1)−N(3)	176.35(7)		165.38(7)	171.28(9)	
N(1)−Co(1)−N(1_1)		176.62(17)			172.0(2)
N(2)−Co(1)−N(3)	96.49(7)		95.93(7)	98.51(8)	
N(2)−Co(1)−N(1_1)		96.96(10)			95.42(15)
N(1)−Co(1)−N(2)	82.07(7)	81.99(10)	80.15(7)	80.05(8)	82.10(15)
N(3)−Co(1)−N(4)	82.17(7)		80.14(7)	79.92(8)	
Co(1)−P(1)−C(37)	118.88(8)	108.0(2)			
Co(1)−P(1)−C(38)	115.32(7)	123.8(2)			
Co(1)−P(1)−C(39)	115.45(8)	120.6(2)			
C(37)−P(1)−C(38)	101.52(11)	99.88(18)			
C(38)−P(1)−C(39)	100.23(10)	100.78(18)			
Co(1)−N(1)−C(4)	113.85(13)	113.74(18)	110.59(13)	112.09(16)	108.3(3)
Co(1)−N(1)−C(1)	139.40(14)	139.9(2)	143.39(15)	141.07(18)	143.6(4)
τ parameter[a]	0.59	0.54	0.33	0.18	0.46

[a] See the definition of τ in ref 17 or in Figure S1 of Supporting Information.

and 1.9214(16) Å) the shortest distances to the metal. In the single case found in the literature of a TBP Co fragment containing two pyrrole units bound to the metal, which is part of a bimetallic Co(III)/U(V) complex,[14] the X-ray structure does not present an axially compressed geometry because the axial pyrrole ligand shows a longer Co−N distance of 2.002 Å and the equatorially bound pyrrole has a Co−N distance of 1.973 Å. The Co1−N1 and Co1−N3 bond distances of complex **3a** are somewhat smaller than those observed in the "parent" tetrahedral $S = 3/2$ complex [Co(κ^2N,N'-$NC_4H_3C(H)$=N-2,6-$^{i}Pr_2C_6H_3$)$_2$] **1e** (1.952(8) −1.985(9) Å), in other [Co(κ^2N,N'-iminopyrrolyl)$_2$] analogue complexes (1.980−1.989 Å),[15] or even in the square planar [Co(κ^2N,N'-$NC_4H_3C(Me)$=N-2,6-$^{i}Pr_2C_6H_3$)$_2$] **1f** (1.9388(13) Å).[6] However, they are within the range of Co−N bonds found in the literature for other Co–pyrrolyl bonds, which are essentially square pyramidal Co(III) porphirinates and corrolates that contain pyrrolyl units bound to Co (1.791−1.979 Å).[16] The remaining three equatorial coordination positions of **3a** are occupied by the two imine nitrogen atoms (N2 and N4) and the phosphorus P1 atom of the PMe_3 ligand, which form an equatorial plane containing the cobalt atom (Δ= 0.016 Å), the sum of the angles around the Co center being virtually 360° (359.98°). However, the N2−Co1−N4 angle (141.24°) is much larger than the other two (P1−Co1−N2, 112.47°; P1−Co1−N4, 106.27°), which is likely a consequence of the repulsion between the bulky imine 2,6-diisopropylphenyl substituents. This leads to a certain extent of distortion of the TBP toward a square pyramidal (SP) geometry, which is pointed out by a τ value of 0.59. The parameter τ[17] (see also definition in Figure S1 of Supporting Information) is used to describe the degree of distortion of penta-coordinated complexes ($\tau = 1$ for an ideal trigonal bipyramid and $\tau = 0$ for an ideal square pyramid).

Higher values of Co−N bond distances are found for the neutral imine nitrogens (Co1−N2 = 2.0483(16) and Co1−N4

(14) Arnold, P. L.; Patel, D.; Blake, A. J.; Wilson, C.; Love, J. B. *J. Am. Chem. Soc.* **2006**, *128*, 9610–9611.

(15) (a) Wei, C. H. *Inorg. Chem.* **1972**, *11*, 1100–1105. (b) Reid, S. D.; Blake, A. J.; Wilson, C.; Love, J. B. *Inorg. Chem.* **2006**, *45*, 636–643.

(16) Results from a search carried out in the Cambridge Structural Database using the program ConQuest, developed by the CCDC.

(17) (a) Addison, A. W.; Rao, T. N.; Reedijk, J.; van Rijn, J.; Verschoor, G. C. *J. Chem. Soc., Dalton Trans.* **1984**, 1349–1356. (b) O'Sullivan, C.; Murphy, G.; Murphy, B.; Hathaway, B. *J. Chem. Soc., Dalton Trans.* **1999**, 1835–1844.

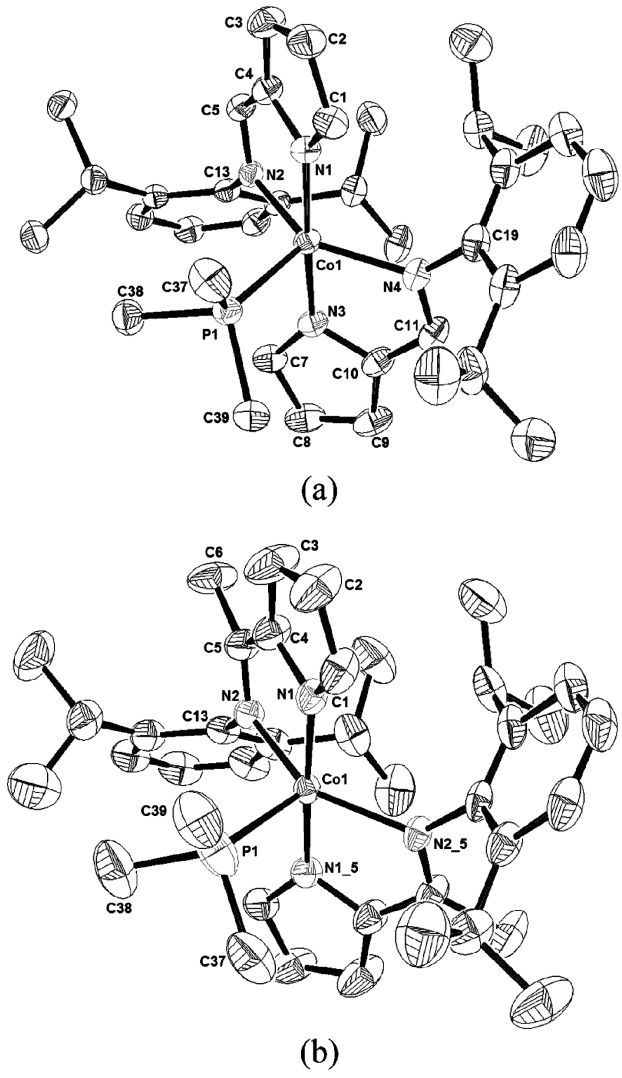

Figure 1. ORTEP III diagram of complexes (a) **3a** and (b) **3b** using 50% probability level ellipsoids. Hydrogens have been omitted for clarity.

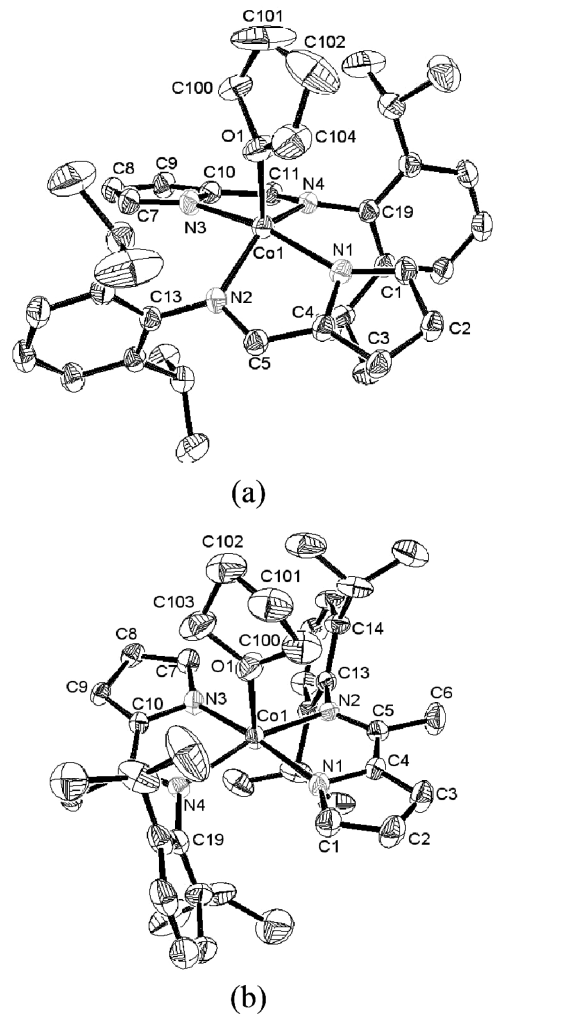

Figure 2. ORTEP III diagram of complexes (a) **4a** and (b) **4b** (from polymorph **4b_I**) using 50% probability level ellipsoids. Hydrogens have been omitted for clarity.

= 2.0481(16) Å) in comparison with the pyrrolyl rings Co−N bond distances. This could be caused by both the anionic nature of the pyrrolyl nitrogen and the steric bulk of the 2,6-diisopropyl substituents of the phenyl rings. Nevertheless, the other examples known in the literature of TBP complexes of Co(II) containing two axial anionic and two equatorial neutral N atoms show longer axial bond lengths.[18] The Co1−N2 and Co1−N4 distances are similar to those found for the imine groups in the tetrahedral complex **1e** (2.034(7)−2.060(8) Å) but considerably larger than those found in the square planar complex **1f** (1.9528(14) Å).[6] The Co1−P1 distance (2.2580(5) Å) lies in the normal range of Co(II)−PMe_3 bond distances.[19,20] Both chelating ligands can be considered planar since the planes defined by N2−C5−C4-N1 and N3−C7−C8−N4, and the respective pyrrolyl rings form angles of 1.29 and 3.41°, respectively. The internal distances and angles observed in the chelating ligands of **3a** and their corresponding bite angles to the Co atom are similar to those found for the tetrahedral **1e** or square planar **1f** complexes.[6]

For complex **3b**, crystals suitable for X-ray diffraction were grown from *n*-hexane solutions. The corresponding molecular structure (Figure 1b) shows the central atom bound to two acetiminopyrrolyl ligands and a disordered PMe_3 coordinated to the fifth coordination site of the metal. The asymmetric unit consists of only half of the complex; the other half was generated by symmetry. As in **3a**, the molecule shows an axially compressed TBP geometry around the cobalt atom, slightly more distorted (τ= 0.54) than **3a**. However, the bond distances and angles are very similar to those found for **3a** despite the C6 and C12 extra methyl groups substituting now the imine C5 and C11 quaternary carbons.

The crystallographic structure of complex **4a** consists of two formiminopyrrolyl ligands coordinated to the Co central atom, which is also coordinated to a molecule of (disordered) THF (Figure 2a and Table 1). The geometry may be interpreted as distorted square pyramidal (τ = 0.33) rather than TBP. The pyrrolyl rings are placed trans to each other

(18) (a) Patra, A. K.; Ray, M.; Mukherjee, R. *J. Chem. Soc., Dalton Trans.* **1999**, 2461–2466. (b) Vickovic, I.; Suste, A.; Falk, H.; Hulita, N. K.; Tonejic, A. M. *Monatsh. Chem.* **1995**, *126*, 971–982.
(19) Alnaji, O.; Peres, Y.; Dartiguenave, M.; Dahan, F.; Dartiguenave, Y. *Inorg. Chim. Acta* **1986**, *114*, 151–158.
(20) Klein, H. F.; Beck, R.; Florke, U.; Haupt, H. J. *Eur. J. Inorg. Chem.* **2003**, 240–248.

with a N1−Co1−N3 axis (165.38(7)°) considerably more distorted from linearity than in **3a** or **3b** (Table 1). The distances Co1−N1 and Co1−N3 of 2.082(18) and 2.0814(18) Å are much larger than those found in complexes **3a** or **3b** ($\Delta \approx 0.17$ Å) or in the related tetrahedral [Co(κ^2*N*,*N*′-$NC_4H_3C(H)$=N-2,6-$^iPr_2C_6H_3$)$_2$] **1e** ($\Delta \approx 0.10 - 0.12$ Å)[6] or square planar [Co(κ^2*N*,*N*′-$NC_4H_3C(Me)$=N-2,6-$^iPr_2C_6H_3$)$_2$] **1f** ($\Delta \approx 0.15$ Å).[6] The remaining two coordination positions in the distorted square plane are occupied by the two imine nitrogen atoms (N2 and N4). The oxygen O1 atom of the THF ligand occupies the apical position of the pyramid, and the cobalt atom is situated above ($\Delta = 0.441$ Å) the basal square plane. Larger Co−N bond distances are found for the imine nitrogens (Co1−N2 = 2.0899(17) Å and Co1−N4 = 2.0942(17) Å) in relation to those of **3a** ($\Delta = 0.0272$ Å), **3b** ($\Delta = 0.0275$ Å), **1f** ($\Delta = 0.1215$ Å),[6] and **1e** (Δ= 0.0155−0.0215 Å).[6] The Co1−O1 distance is 2.0487(17) Å, which lies in the normal range of Co(II)−THF bond distances (1.876−2.225 Å; average = 2.09)[16] but is lower than the other bonds in the equatorial plane, indicating a compressed SP-geometry. The chelating ligands can be considered planar because the angle defined by (N1−C4−C5−N2) and the pyrrolyl ring is 0.82° (and by N3−C10−C11−N4 and the other pyrrolyl ring is 1.35°). The internal distances and angles observed in the chelating ligands of **4a** and their corresponding bite angles to the Co atom are similar to those found for the tetrahedral complexes **3a**, **3b**, **1e**,[6] and **1f**.[6] The fact that all the Co−N distances have expanded in relation to complex **3a** corroborates the results obtained by magnetic moment measurements in the solid state (see below) that indicate the complex **4a** has a high-spin ground state ($S = 3/2$), rather than a low-spin ground state (S=1/2), found for complex **3a**.

Crystals of compound **4b** suitable for X-ray diffraction were obtained either in the synthesis of **4b** via the synthetic method indicated in Scheme 4 (monoclinic polymorph **4b_I**) or, as a byproduct, in the synthesis attempts of **3b** in THF (tetragonal polymorph **4b_II**). The molecular structure of the monoclinic polymorph **4b_I** consists of two acetiminopyrrolyl ligands coordinated to a Co central atom, which is also coordinated to a molecule of THF (Figure 2b and Table 1). Its geometry can also be interpreted as distorted square pyramidal ($\tau = 0.18$), but some of the structural data, mainly related to the metal atom, are considerably different from those of **4a**. As the Co1−O1 bond of **4b_I** (2.014(2) Å) is longer ($\Delta = 0.055$ Å), the Co1−N1 and Co1−N2 belonging to the same bidentate ligand have, respectively, a significant increase ($\Delta = 0.0546$ Å) or decrease (Δ= 0.068 Å) in relation to **4a**. The angle formed between the Co atom and the imine nitrogens, N2−Co1−N4 (160.45(8)°), increase by 14.81°, whereas that involving the pyrrolyl nitrogens, N1−Co1−N3 (171.28(8)°), increase by ∼6°.

The molecular structure of the polymorph **4b_II** shows the cobalt atom coordinated to two acetiminopyrrolyl ligands in a distorted square pyramidal arrangement, with a THF molecule coordinated to the fifth coordination site of the metal. The asymmetric unit consists of only half of the complex; the other half-was generated by symmetry (see Figure S4 Supporting Information and Table 1). The geometry of **4b** in polymorph **4b_II** can be interpreted as a considerably distorted SP geometry ($\tau = 0.46$). However, because the Co1−O1 bond length (2.182(12) Å) is much longer than those found in **4a** ($\Delta = 0.134$ Å) or **4b_I** ($\Delta = 0.079$ Å), the molecules of polymorph **4b_II** can be considered to be in an elongated square pyramidal geometry, with the distances and angles in the equatorial plane relatively similar to those of **4a**; this Co1−O1 bond length still lies in the normal range of Co(II)−THF bond distances (1.876−2.225 Å; average = 2.09).[16]

Table 2. Effective Magnetic Moments μ_{eff} (μ_B) for Complexes **3a**, **b** and **4a**,**b**, Measured in Powder (DC Extraction and SQUID Methods) and in Toluene Solution (Evans Method-NMR), at 300 K

	solid state	solution
complex	μ_{eff} (μ_B)	μ_{eff} (μ_B)
3a	2.03[b]	2.31
3b	1.98[b]	2.61
4a	4.87[c]	1.76
4b[a]	4.87[c]	1.78

[a] The sample measured corresponds to polymorph **4b_I**. [b] DC extraction method. [c] SQUID method.

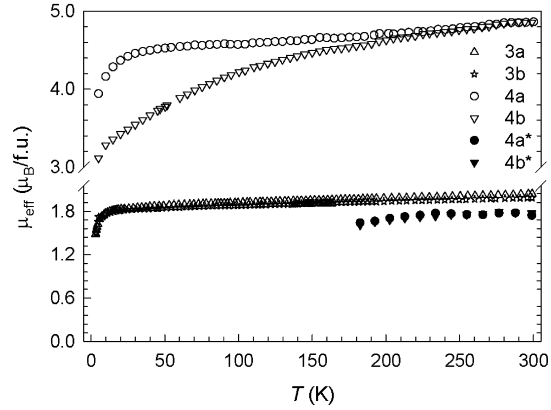

Figure 3. Temperature dependences of the effective magnetic moment μ_{eff} of complexes **3a**, **3b**, **4a**, and **4b** (from polymorph **4b_I**), taken in the solid state, at 5 T (white experimental points) and taken in toluene solutions of compounds **4a** and **4b**, by the Evans method (black experimental points).

Magnetic Measurements. The results obtained for the magnetic susceptibility measurements of the different complexes, taken both in toluene solution (by Evans method-NMR) and in powder (DC extraction method for **3a**, **b** and SQUID magnetometer for **4a**, **b**), at 300 K, are summarized in Table 2.

The temperature dependence of the effective magnetic moment, μ_{eff}, obtained for polycrystalline powder samples of complexes **3a**, **3b**, **4a**, and **4b** (from polymorph **4b_I**) is presented in Figure 3. For samples **3a** and **3b**, the decrease of the magnetic moment at lower temperatures (T < 10 K) is a consequence of the high field employed in the measurements (5 T).

The μ_{eff} data taken at 300 K and presented in Table 2 show that the magnetic moments of compounds **3a** and **3b**, obtained in solid and solution phases, are close to the expected spin-only value for low-spin $S = 1/2$ complexes (1.73 μ_B), in agreement with the EPR data obtained in toluene presented below. The small differences on the values

obtained by these two methods are very common, normally caused by several factors, such as the local geometry or the different calculation methods inherent to each technique.[21] In this case, the μ_{eff} obtained by the Evans method were 2.3 and 2.6 μ_B for **3a** and **3b**, respectively, which still lie in the typical range observed for trigonal bipyramidal Co(II) complexes with low-spin ground states with $S = 1/2$ (2.1−2.9 μ_B).[22,23] The high temperature range data (100−300 K) obtained for solid samples of **3a** and **3b** (DC extraction method) fit well to the Curie−Weiss law, giving negative values for the Weiss constants, $\theta = -16.9$ and -22.3 K, respectively. This indicates the presence of antiferromagnetic exchange interactions in the solid state between adjacent Co(II) ions (see Figure S5, Supporting Information).

For both complexes **4a** and **4b** (polymorph **4b_I**), the magnetic moments measured in the solid state (SQUID method) were 4.87 μ_B, at room temperature, (Table 2 and Figure 3). This value lies in the range observed for Co(II) complexes with high-spin ground state,[22] although it is much larger than the spin-only magnetic moment value of 3.87 μ_B ($S = 3/2$), which indicates that some significant orbital contribution from low energy excited states can be involved. The fitting of the high temperature range magnetic susceptibility data of **4a** (150−300 K) and **4b** (100−300 K) to the Curie−Weiss law (see Figure S6, Supporting Information) also reveals the presence of antiferromagnetic interactions between adjacent Co(II) ions, the values for the Weiss constants ($\theta = -41.6$ and -59.8 K, respectively) being more negative than those of **3a**, **b**. Concerning complex **4b**, it should be emphasized that the only sample analyzed was polymorph **4b_I** because crystals of polymorph **4b_II** have only been obtained once, but in a mixture with compound **3b** (see Synthesis of Complexes and X-ray Diffraction). Therefore, the magnetic moment of polymorph **4b_II** has not been measured, and the spin state of its molecules is unknown. The exchange pathway for these antiferromagnetic interactions can be inferred from the short contacts found in the molecular packing. In fact, for **4a**, the distance between the outmost carbons of two phenyl rings in neighboring molecules is about 3.34 Å, favoring some $\pi\cdots\pi$ interactions, and for **4b** (in polymorph **4b_I**), in spite of the intrinsic disorder, several short contacts can be noticed between pyrrole rings of neighboring units (C−H$\cdots\pi$ interactions, ∼2.62 Å) and between THF methylene hydrogens with pyrrole rings (C−H$\cdots\pi$ interactions, ∼2.89 Å) or isopropyl methyl groups of (C−H$\cdots$C interactions, ∼2.87 Å) of adjacent molecules (Figures S7 and S8, Supporting Information).

Unexpectedly, the magnetic moments of complexes **4a** and **4b** (polymorph **4b_I**) measured in solution by the Evans method, at room temperature, 1.76 and 1.78 μ_B, respectively (Table 2), are much lower than those obtained in the solid state, being very close to the spin-only magnetic moment value for low-spin complexes with $S = 1/2$. Furthermore, variable-temperature Evans method measurements on these compounds reveal that their μ_{eff} is approximately invariant with temperature (Figure 3), suggesting that the observed numerical change in the μ_{eff} from the solid state to solution could not be associated with any equilibrium between species with different spin ground states. In addition, the aforementioned antiferromagnetic interactions (rather than ferromagnetic ones) observed in **4a** and **4b** rule out the presence of μ_{eff}magnifying effects caused by solid state cooperative effects. The influence of different environments, such as solution and solid state, may strongly influence the stereoelectronic properties of the ligands, either because of polar effects or, indirectly, by controlling the ligands' conformation.[21,24]

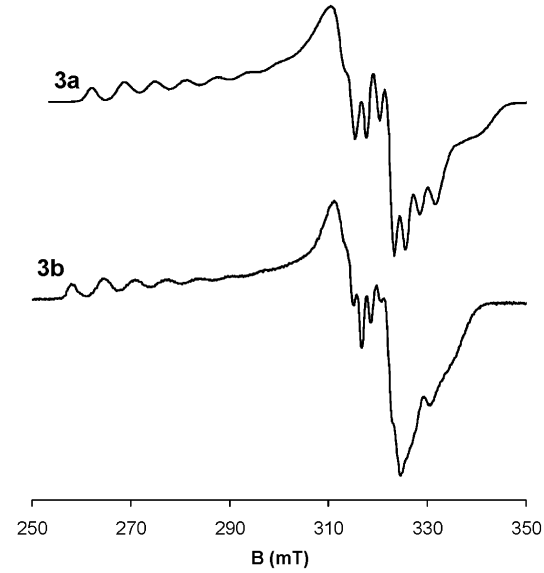

Figure 4. EPR spectra of complexes **3a** and **3b**, in toluene, at 77 K.

To obtain further information on the electronic structure of all Co(II) complexes, including an explanation for the abrupt change in the spin ground-state of complexes **4a** and **4b** from the solid state to solution, EPR spectra of all complexes, were obtained in frozen toluene solution.

EPR Spectra. The experimental EPR spectra of complexes **3a** and **3b** and **4a** and **4b**, obtained at 77 K, are depicted in Figures 4 and 5, respectively. Complexes of types **a** and **b** show almost identical EPR spectra, indicating that the two different substituents (R = H and Me) of the imine bond in the bidentate ligand do not have a significant influence in the electronic structure of the cobalt center. In frozen toluene solution, the spectra are of axial (complexes **3**) and rhombic (complexes **4**) types and with large tensor anisotropy, g_{av} in the range of 2.2−2.4, ($[g_{av} = (2g_{1,2} + g_3)/3]$, where $g_{1,2}$ and g_3 refer to the lowest and highest magnetic field g values, respectively), and typical of low-spin cobalt(II) complexes

(21) de Buysser, K.; Herman, G. G.; Bruneel, E.; Hoste, S.; van Driessche, I. *Meas. Sci. Rev.* **2005**, *5*, 30–33.
(22) Lever, A. B. P. *Inorganic Electronic Spectroscopy*; Elsevier: Amsterdam, 1968.
(23) Kennedy, B. J.; Fallon, G. D.; Gatehouse, B. M. K. C.; Murray, K. S. *Inorg. Chem.* **1984**, *23*, 580–588.
(24) Wolny, J. A.; Rudolf, M. F.; Ciunik, Z.; Gatner, K.; Wolowiec, S. *J. Chem. Soc., Dalton Trans.* **1993**, 1611–1622.

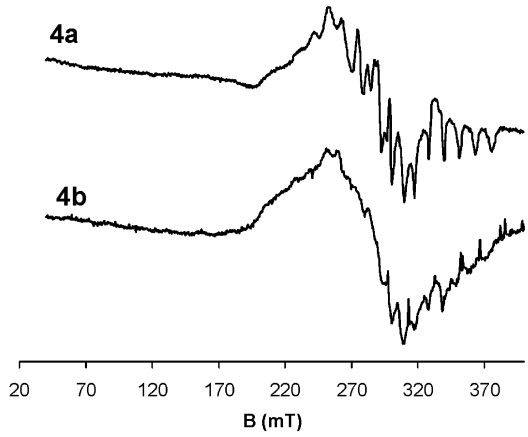

Figure 5. EPR spectra of complexes **4a** and **4b** (polymorph **4b_I**), in toluene, at 77 K.

(d^7) with $S = 1/2$.[25] However, complexes **3** and **4** exhibit EPR spectra with different *g* patterns and hyperfine/superhyperfine splittings in the high and low magnetic field regions, anticipating different geometries and, consequently, different electronic ground states for complexes **3** and **4**. The first important conclusion obtained from the EPR data is their full agreement with the results obtained by the magnetic moment measurements in solution (by the Evans method) for all the compounds, in particular, for complexes **4a** and **4b**.

The observed *g* patterns and hyperfine/superhyperfine splittings are similar to other low-spin pentacoordinated cobalt(II) complexes,[25] and in the absence of EPR crystal data for complexes **3** and **4**, these similarities can be further extended to support the following orientation scheme for the tensor axis in these cobalt complexes: for complex **3a** and **3b**, EPR parameters in the high and low field regions correspond to parallel and perpendicular parameters, respectively, whereas for complexes **4a** and **4b** the assignment of the EPR parameters is the opposite. In this context, for complexes **3a** and **3b**, $g_{1,2} = g_{||} > g_3 = g_\perp$, and $|A_{1,2}|^{Co} = |A_{||}|^{Co} > |A_3|^{Co} = |A_\perp|^{Co}$, but for complexes **4a** and **4b**, $g_{1,2} = g_{xy} > g_3 = g_z$, and $|A_{1,2}|^{Co} = |A_{xy}|^{Co} > |A_3|^{Co} = |A_z|^{Co}$. The EPR parameters obtained from spectra simulation are summarized in Table 3.

The *g* and *A* Co patterns observed in the spectra of complexes **3a** and **3b**, namely, $g_{||} > g_\perp$ $|A_{||}|^{Co} > |A_\perp|^{Co}$, as well as their values, are typical of cobalt(II) complexes with compressed trigonal bipyramidal geometry with a $d_{x^2-y^2}/d_{xy}$ ground state,[25] indicating that the solid state geometry, obtained by X-ray diffraction, has been kept in toluene solution. In the parallel region (higher magnetic field region), the hyperfine splittings caused by the interaction between the metal unpaired electron and the cobalt center ($|A_{||}|^{Co} = 6.2 - 6.5$ mT; $I(Co) = 7/2$) are clearly seen. The perpendicular region is of more difficult interpretation, but the observed superhyperfine splittings are compatible with an interaction of the unpaired electron with the phosphorus nucleus of the coordinated PMe_3 ($|a_\perp|^P = 7.0 - 8.5$ mT, $I(P) = 1/2$), and further splitting of these signals is caused by the presence of two equivalent imine nitrogen atoms of the bidentate ligands located in the equatorial plane; a nice well resolved quintuplet is clearly seen in the perpendicular region of complex **3b** spectrum ($|a_\perp|^N = 2.0 - 2.7$ mT; $I(N) = 1$).[25] The EPR results also confirm that not only the geometry of complexes **3a** and **3b** have been kept in toluene solution, but also that no ligand intramolecular fluxionality is occurring because the coordinated atoms kept their positions within the trigonal bipyramid.

For complexes **4a** and **4b**, the observations of $g_{xy} > g_z$ and $|A_{xy}|^{Co} > |A_z|^{Co}$, indicate the complexes have a different ground-state and geometry of those of complexes **3a** and **3b**. These previous observations, along with the absolute values obtained for *g* and *A* parameters, are consistent with a square pyramidal geometry, although with axial elongation, for both complexes **4a** and **4b**, which lead to d_{z2} ground states. Although the spectra do not have very good resolution, in part because of the extensive overlap between the *xy*- and *z*-regions, it is possible to see in the g_z region the majority of the eight predicted cobalt hyperfine splittings caused by the interaction of the unpaired spin and the metal center ($|A_z|^{Co} = 10.5 - 11.0$ mT; $I(Co) = 7/2$). The absence of any additional superhyperfine splittings in the previous cobalt features further indicates that the axial position of the square pyramid has to be occupied by the THF molecule, which coordinates to Co through the oxygen atom ($I = 0$ for the isotope with higher natural abundance). In this context, this Co−O bond will have a larger bond length compared to any of the Co−N bonds within the equatorial plane. In the *xy*-region, the observed nonresolved hyperfine couplings are caused by the interaction of the unpaired spin with the cobalt atom but no superhyperfine splittings because the coordinating atoms from the equatorial ligands are usually seen for this type of ground state (d_{z2}) since the spin interaction mechanisms would be of indirect nature (polarization), thus being of very small magnitude.[25b,d]

The EPR results for complexes **4a** and **4b** are partially in disagreement with the structural data from X-ray diffraction because they suggest, for both complexes, axially elongated square pyramidal geometries, with consequent low-spin ground states. As seen in the last section, both complexes exhibit, in the solid state, magnetic moments compatible with high-spin ground states which are in accordance with the X-ray data. Nevertheless, in toluene solution the magnetic moments suggest a low-spin ground state, but do not provide a structural rationalization for the change in the spin state of the complex. Herein, EPR data definitely confirms the change in the spin ground-state to low-spin in toluene solution, further indicating the same square pyramidal geometry for complexes **4a** and **4b**, although with different axial distortions. Therefore, the magnetic behavior exhibited by complexes **4a** and **4b**, reflecting different spin ground states in solid state and solution, is attributed to a relaxation of the compressed geometry of complexes **4**, upon dissolution

(25) (a) Daul, C.; Schläpfer, C. W.; von Zelewsky, A. *Struct. Bonding (Berlin)* **1979**, *36*, 129–171. (b) McGarvey, B. R. *Can. J. Chem.* **1975**, *53*, 2498–2511. (c) Malatesta, V.; McGarvey, B. R. *Can. J. Chem.* **1975**, *53*, 3791–3800. (d) Hitchman, M. A. *Inorg. Chem.* **1977**, *16*, 1985–1993. (e) Nishida, Y.; Kida, S. *Bull. Chem. Soc. Jpn.* **1972**, *45*, 461–465. (f) Nishida, Y.; Ida, K.; Kida, S. *Inorg. Chim. Acta* **1980**, *38*, 113–116.

Table 3. EPR Parameters for Complexes **3a**, **3b**, **4a**, and **4b** (Polymorph **4b_I**)

complex	$g_{\|\|}$	$g_\perp$[a]	$\|A_{\|\|}\|^{Co}$ (mT)	$\|A_\perp\|^{Co}$ (mT)[a]	$\|a_{\|\|}\|^{P}$ (mT)	$\|a_\perp\|^{P}$ (mT)[a]	$\|a_{\|\|}\|^{N}$ (mT)	$\|a_\perp\|^{N}$ (mT)[a]
3a	2.38	2.11	6.2	0.5	1.5	8.5	0.5	2.7
3b	2.41	2.13	6.5	0.5	1.5	7.0	0.5	2.0

complex	g_x[a]	g_y[a]	g_z	$\|A_x\|^{Co}$ (mT)[a]	$\|A_y\|^{Co}$ (mT)[a]	$\|A_z\|^{Co}$ (mT)
4a	2.60	2.45	2.00	7.0	6.0	11.0
4b	2.65	2.35	2.05	6.5	6.0	10.5

[a] The values are not accurate. See experimental section for details.

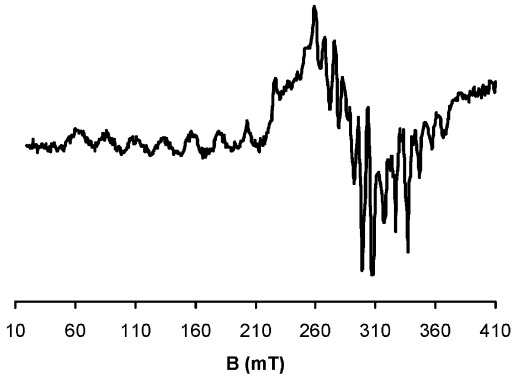

Figure 6. EPR spectrum of complex **1f**, in toluene, at 77 K.

in toluene, through an elongation of the Co−O bond length. This increase leads to a modification in the ratio between the equatorial and axial ligand fields, ultimately changing the spin ground-state of the complexes. Further insights into the different available geometries and ground states for complexes **3** and **4** were also analyzed by DFT calculations (see below).

Compound **1f**, obtained as a byproduct on the attempted synthesis of **3b** in THF, and already structurally characterized in a previous work as a complex with a low-spin ($S = 1/2$) ground state,[6] was also characterized by EPR spectroscopy in frozen toluene solution (Figure 6). The spectrum is of the rhombic type with a very large tensor anisotropy, $g_1 = 4.60$, $g_2 = 2.32$, and $g_3 = 1.97$ ($g_{av} = 2.96$), with g_1 and g_3 corresponding to the lowest and highest magnetic field g values, respectively, which are typical of Co(II) low-spin square planar complexes with a $d_{x^2-y^2}/d_{xy}$ ground state,[25a,d] confirming the results described in ref 6. The spectrum also shows in all g regions well resolved hyperfine splittings because of the interaction between the unpaired spin and the cobalt center ($I(Co) = 7/2$), whose coupling constants corroborate the square planar geometry: $|A_1|^{Co} = 24$ mT, $|A_2|^{Co} = 7.8$ mT, and $|A_3|^{Co} = 7.8$ mT. Although no well-resolved superhyperfine splittings resulting from the four equivalent nitrogens from the equatorial ligands could be detected in any of the g regions, the simulation of the spectrum was made taking with account the following nitrogen coupling constants: $|a_1|^{N} = 2.2$ mT and $|a_{2,3}|^{N} = 1.0$ mT; $I(N) = 1$.

DFT Calculations. The relative stability of the two different spin ground states ($S = 3/2$ and $S = 1/2$) for both complexes with PMe_3 (**3a** and **3b**) and THF (**4a** and **4b**) was investigated by means of DFT calculations.[26]

The optimized geometries calculated for complexes **3a** and **3b** are presented in Figure 7. Their structures correspond to distorted and axially compressed trigonal bipyramidal geometries, in accordance with the X-ray results. The pyrrolyl nitrogen atoms occupy the axial positions, while the phosphorus and the two imine nitrogen atoms occupy the equatorial plane. The agreement between calculated and experimental structures can be evaluated by the mean (δ) and maximum (Δ) absolute deviations obtained for the coordination distances (Co−X). For the low-spin form of complex **3a**, values of $\delta = 0.08$ Å and $\Delta = 0.18$ Å indicate a poor agreement. The geometry optimized for complex **3b** ($S = 1/2$) present similar values: $\delta = 0.09$ Å and $\Delta = 0.19$ Å. In both cases, the Co−P bond is grossly overestimated, corresponding to the maximum deviation referred above (Δ). The values obtained for the Co−N distances are comparatively better, with overestimations of about 0.02 and 0.09 Å, for the pyrrolyl and the imine nitrogen atoms, respectively. The size and complexity of the molecules prevent the use of higher theory level methods and bigger basis sets for the geometry optimizations (see Computational Details). Since similar deviations are observed for the Co-X coordination distances in both complexes, **3a** and **3b**, the results obtained may be used in the comparative study of these two molecules presented below.

The complexes with the low-spin ground state ($S = 1/2$) correspond to the more stable species for complexes **3a** and **3b**, in good agreement with the solution EPR spectra, the experimental magnetic susceptibility measurements in both solid state and solution (see Tables 2 and 3), and the X-ray structural data (e.g., τ values, see Table 4). A significant expansion of about 0.1 Å is observed for all coordinative distances, Co−X, going from the low- to the high-spin ($S = 3/2$) complexes, similar to what has been observed in related Co(II) complexes.[6,9]

The different behavior of the two complexes, **3a** and **3b**, in the presence of THF was studied through the calculation of the energy balance for the addition of PMe_3 to the parent [Co(2-iminopyrrolyl)$_2$] complexes, **1e** and **1f**. The free energy values presented in Scheme 5 include solvation effects (THF), taken into account by means of the PCM model (see Computational Details). The values obtained for the formation of complexes **3a** and **3b** show a moderately favorable reaction ($\Delta G = -1.3$ and -2.5 kcal/mol, respectively) and, being similar for both species, suggest that there is no thermodynamic reason for the observed differences. Thus, the instability of **3b** in THF is probably a consequence of kinetic factors.

The THF complexes (**4a** and **4b**) were also the subject of geometry optimizations, and the calculated structures are represented in Figure 8.

(26) Parr, R. G.; Yang, W. *Density Functional Theory of Atoms and Molecules*; Oxford University Press: New York, 1989.

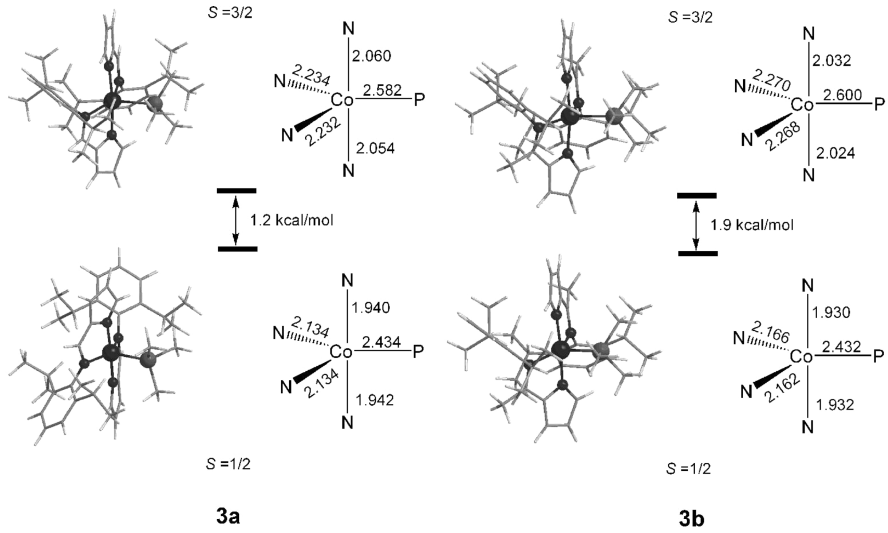

Figure 7. Optimized geometries (B3LYP) for the high-spin ($S = 3/2$, top) and the low-spin ($S = 1/2$, bottom) ground states of complexes **3a** and **3b**. The relative energy (gas phase) of both ground states (kcal/mol), and the coordination distances (Co-X, Å), are presented.

Table 4. Comparison of Experimental (X-ray Diffraction) and Calculated (DFT) Structural Parameter τ of Complexes **3a**, **3b**, **4a**, and **4b**[a]

complex	τ_{exp}	τ_{calcd} $S = 1/2$	τ_{calcd} $S = 3/2$
3a	0.59	0.49	0.46
3b	0.54	0.53	0.44
4a	0.33	0.25	0.31
4b	0.18 (**4b_I**), 0.46 (**4b_II**)	0.30	0.41

[a] See the definition of τ in ref 17 or in Figure S1 of Supporting Information.

Scheme 5

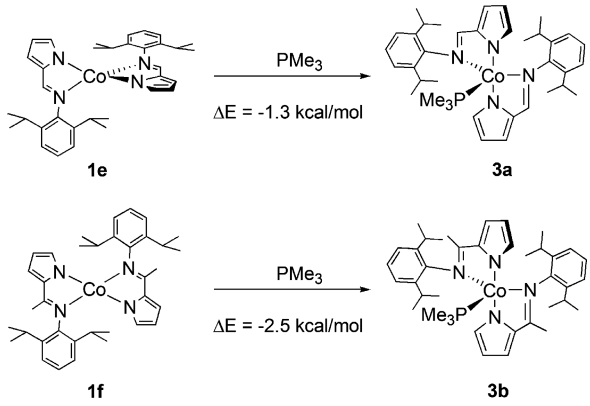

The geometries calculated for the THF complexes (**4a** and **4b**) agree with the corresponding X-ray determined structures, being closer to square pyramidal arrangements discussed above (see τ values in Table 4). The agreement between experimental and calculated Co−X bond distances is better for the THF species ($S = 3/2$) than for the PMe_3 complexes, as demonstrated by smaller values of the maximum and mean absolute deviations: $\Delta = 0.10$ and $\delta = 0.06$ Å for **4a**, and $\Delta = 0.09$ and $\delta = 0.06$ Å for **4b** (comparing with the X-ray structure of polymorph **4b_I**).

For the THF complexes the high-spin ground state ($S = 3/2$) is more stable than the low-spin ground state ($S = 1/2$), showing a reversed stability order, compared with the phosphine derivative complexes, **3a** and **3b**. Curiously, this result, obtained from gas phase energy calculations (see Computational Details), is in agreement with the solid state magnetic susceptibility measurements (see Table 2), suggesting that the X-ray structures determined for **4a** and **4b** should correspond to the complexes with high-spin ground states. It should be noticed that the relative stability calculated in the gas phase for the two spin ground states of complexes **4a**, **b** (see Figure 8) is maintained if dielectric solvent effects are taken into consideration (toluene, PCM model). On the other hand, the Co−O distances calculated for the low-spin ground-state complexes **4a** and **4b** are ~0.2 Å longer than the corresponding molecules with high-spin ground states, representing the larger difference in coordination distances between spin ground states. The resulting geometry of the low-spin complexes **4a** and **4b** correspond to a square pyramid axially elongated along the Co−O bond, in excellent agreement with the EPR results (see above).

The reason for the reversed stability calculated in the gas phase for the complexes **4a** and **4b** with different spin ground states, when compared with complexes **3a** and **3b**, can be traced to the nature of the corresponding ligands, THF and PMe_3, respectively. In fact, the phosphine is a much better σ donor and, thus, a stronger ligand than THF.[10c] The Co−P bonds in the low-spin complexes **3a**, **b** are longer than the Co−O bond distances in **4a**, **b** ($S = 3/2$), but the former correspond to stronger bonds, as shown by the corresponding Wiberg indices[27] (WI): 0.332(**3a**)/0.342(**3b**) and 0.080(**4a**)/0.081(**4b**), respectively.[28] The charge on the metal[29] shows

(27) (a) Wiberg, K. B. *Tetrahedron* **1968**, *24*, 1083–1096. (b) Wiberg indices are electronic parameters related to the electron density between atoms. They can be obtained from a Natural Population Analysis and provide an indication of the bond strength.

(28) The comparison was made between the more stable spin isomers of complexes **3a-b** and **4a-b**, that is, the $S = 1/2$ and 3/2 species, respectively. However, the trend is maintained if the other isomers are considered: $WI_{Co-P} = 0.231$(**3a**, $S = 3/2$)/0.224(**3b**, $S = 3/2$), $WI_{Co-O} = 0.040$(**4a**, $S = 1/2$)/0.056 (**4b**, $S = 1/2$).

(29) Obtained by means of a Natural Population Analysis (NPA).

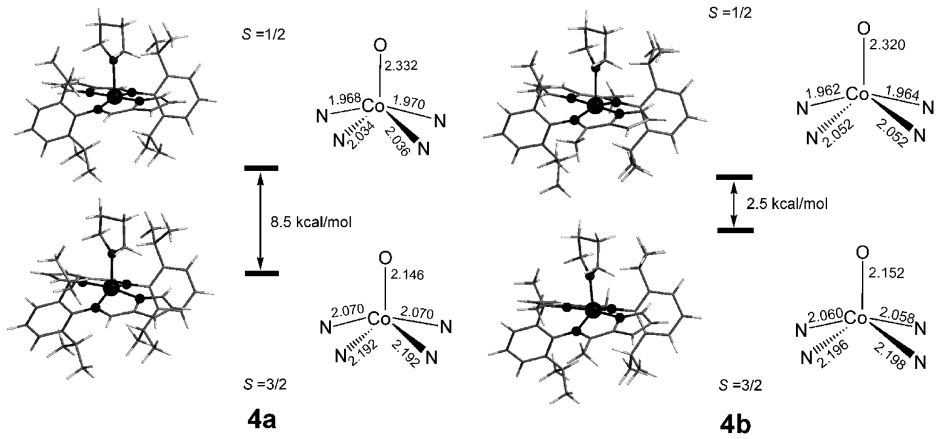

Figure 8. Optimized geometries (B3LYP) of the low- ($S = 1/2$, top) and the high-spin ($S = 3/2$, bottom) ground states of complexes **4a** and **4b**. The relative energy (gas phase) of both ground states (kcal/mol) and the coordination distances (Co−X, Å) are presented.

the same trend: a stronger bond and a better donor in **3a**, **b** is associated with an electron richer metal. This trend is verified for both the high- and the low-spin complexes.[30]

The spin density calculated for the low-spin ($S = 1/2$) complex **3a** is centered on the bipyramidal trigonal xy equatorial plane (Figure 9a), while that of the low-spin ($S = 1/2$) complex **4a** is distributed along the square pyramidal Co−O apical axis (Figure 9b), being their shapes reminiscent of the $d_{x^2-y^2}/d_{xy}$ and d_{z^2} orbitals, respectively. This result is in excellent agreement with the frozen solution EPR spectra (see above) that revealed $d_{x^2-y^2}/d_{xy}$ and d_{z^2} low-spin ground states for **3a** and **4a**, respectively. The spin densities calculated for the low-spin complexes **3b** and **4b** (see Figure S12, Supporting Information) are almost identical to those of the corresponding **3a** and **4a** complexes, also in agreement with the EPR data.

Conclusions

The new bis-iminopyrrolyl five-coordinate Co(II) complexes [Co(κ^2*N*,*N*′-NC_4H_3C(R)═N-2,6-$^i Pr_2C_6H_3$)$_2$(PMe_3)] (R= H **3a**; Me **3b**) may be synthesized in high yields, using THF and diethyl ether as solvents, respectively, by the (a) treatment of $CoCl_2(PMe_3)_2$ with the corresponding iminopyrrolyl Na salts (**Ie** or **If**) or (b) reaction of anhydrous $CoCl_2$ and PMe_3 with **Ie** or **If**. A third route was attempted, involving the addition of excesses of PMe_3 to the tetrahedral and square planar complexes **1e** and **1f**, respectively, [Co(κ^2*N*,*N*′-NC_4H_3C(R)═N-2,6-$^i Pr_2C_6H_3$)$_2$] (R = H **1e**; Me **1f**), being only successful for the low yield synthesis of **3a**, because of the difference in hindrance of the formimino and acetiminopyrrolyl ligands. The synthesis of **3b** in THF is unfruitful because of the kinetic competition of the solvent, giving rise to mixtures of **1f** and its coordinated THF adduct **4b**.

The synthesis of the new bis-iminopyrrolyl five-coordinate Co(II) complexes [Co(κ^2*N*,*N*′-NC_4H_3C(RH)═N-2,6-$^i Pr_2C_6H_3$)$_2$(THF)] (R = H **4a**; Me **4b**) was carried out in high yields by the reaction of $CoCl_2(THF)_{1.5}$ with the corresponding iminopyrrolyl Na salt.

(30) Calculated Co NPA charges: 1.23 (**3a** $S = 1/2$), 1.23 (**3b** $S = 1/2$), 1.30 (**4a** $S = 1/2$), 1.30 (**4b** $S = 1/2$), 1.47 (**3a** $S = 3/2$), 1.49 (**3b** $S = 3/2$), 1.57 (**4a** $S = 3/2$), 1.58 (**4b** $S = 3/2$).

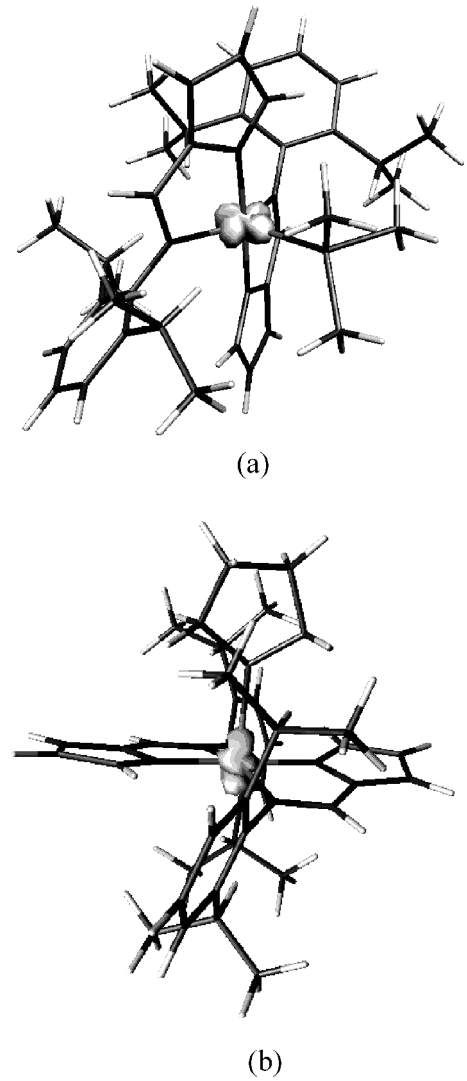

Figure 9. Spin densities calculated (B3LYP) for the low-spin ground states ($S = 1/2$) of complexes (a) **3a** and (b) **4a**.

All the compounds have been characterized by X-ray diffraction, with **3a** and **3b** showing axially compressed trigonal bipyramidal geometries, whereas **4a** and **4b** show distorted square pyramidal ones, with axially compressed (**4a** and polymorph **4b_I**) or elongated (polymorph **4b_II**) forms. Magnetic measurements either in the solid or in the liquid

states indicate that complexes **3a** and **3b** have low-spin ground states ($S = 1/2$). However, compounds **4a** and **4b** behave unusually since they show magnetic moments compatible with high-spin ground-state complexes ($S = 3/2$) in the solid state, but in toluene solutions, they match with spin-only values for low-spin ground state ($S = 1/2$) complexes. This behavior is confirmed by EPR spectroscopy, and can be assigned to an elongation of the Co−THF bond that occurs upon toluene dissolution. Such type of changes in the metal−ligand bond lengths can easily occur for weak ligands, such as THF.

Experimental Section

General Considerations. All experiments dealing with air- or moisture-sensitive materials were carried out under inert atmosphere using a dual vacuum/nitrogen line and standard Schlenk techniques. Nitrogen gas was supplied in cylinders by Air Liquide and purified by passage through 4 Å molecular sieves. Unless otherwise stated, all reagents were purchased from commercial suppliers (e.g., Acros, Aldrich, Fluka) and used without further purification. All solvents were used under inert atmosphere and thoroughly deoxygenated, dried, and purified by refluxing over a suitable drying agent, followed by distillation under nitrogen. The following drying agents were used: sodium (for toluene, diethyl ether and tetrahydrofuran) and calcium hydride (for *n*-hexane). Deuterated solvents were dried by storage over 4 Å molecular sieves and degassed by the freeze−pump−thaw method. Solvents and solutions were transferred using a positive pressure of nitrogen through stainless steel cannulae and mixtures were filtered in a similar way using modified cannulae that could be fitted with glass fiber filter disks.

The ligand precursors (2,6-diisopropyl-phenyl-(1*H*-pyrrol-2-yl-methylene)-amine) and (2,6,-diisopropyl-phenyl-[1-(1*H*-pyrrole-2-yl)-ethylidene]-amine) and their corresponding sodium salts, respectively, **Ie** and **If**, were prepared according to our previous work.[6,7] The syntheses of $CoCl_2(PMe_3)_2$,[31] $CoCl(PMe_3)_3$,[32] and $[Co_4Cl_8(THF)_6]$ $(CoCl_2(THF)_{1.5})$[12c] were adapted from the literature. The syntheses of complexes $[Co(\kappa^2N,N'\text{-}NC_4H_3C(R)=N\text{-}2,6\text{-}{}^iPr_2C_6H_3)_2]$ (R = H **1e**, Me **1f**) were performed as described in the literature.[6]

Nuclear magnetic resonance (NMR) spectra were recorded on Varian Unity 300 MHz or Bruker Avance III 300 spectrometers, at 299.995 and 300.13 MHz (^1H), and were referenced internally using the residual protio solvent resonance relative to tetramethylsilane (δ=0). For air- and -moisture sensitive materials, samples were prepared in a glovebox, in J. Young NMR tubes, using toluene-d_8 (magnetic susceptibilities measurements by the Evans method).

Elemental analyses were obtained from the IST or ITN elemental analysis service.

Mass spectra were collected on a 500 MS LC Ion Trap (Varian, Inc., Palo Alto, CA, USA) mass spectrometer equipped with an ESI source. The spray voltage was set at ± 5 kV and the capillary voltage was set at 10 V.

EPR spectra were obtained using an X-band Bruker ESP300E spectrometer equipped with a microwave bridge ER033, a rectangular cavity operating in the T102 mode and a NMR gaussmeter ER = 35M. The modulation amplitude was kept well below the line width and the microwave power well below saturation. A finger-quartz cryostat with liquid nitrogen was used for acquiring the spectra at 77 K. Samples were prepared in a glovebox, by dissolving the complexes in freshly distilled toluene and filtering the solutions to EPR tubes. The reported EPR parameters were obtained by simulation of the experimental spectra using the program WinEPR Simfonia (Bruker) assuming axial spin Hamiltonians for complexes **3** and rhombic ones for complexes **4** and **1f**. For all complexes, the *g* and *A* parameters in the perpendicular/xy regions, are less accurate because of their dependence on the line widths (1.5−2.0 mT for complexes **3** and 2.0−5.0 mT for complexes **4**) used in the simulations and low spectral resolution.

Synthesis of $[Co(\kappa^2N,N'\text{-}NC_4H_3C(H)=N\text{-}2,6\text{-}{}^iPr_2C_6H_3)_2(PMe_3)]$ (3a). Method a. NaH (48 mg, 2 mmol) was suspended in tetrahydrofuran, and 2 mmol (0.508 g) of the neutral formiminopyrrole ligand precursor was slowly added as a solid, under a counterflow of nitrogen. The resulting orange-brown solution was filtered and added dropwise to a previously cooled (−78 °C) suspension of $CoCl_2(PMe_3)_2$ (0.253 g, 1 mmol) in tetrahydrofuran. This mixture was stirred for an hour and then allowed to cool to room temperature. After 2 h, all volatiles were evaporated under vacuum, and the residue was extracted with *n*-hexane until extracts remained colorless. The resulting orange-brown solution was concentrated and cooled to −20 °C to yield 0.627 g (98%) of dark red crystals. Crystals suitable for X-ray diffraction were obtained. This reaction was also carried out using a 1:1 stoichiometric ratio of ligand/metal yielding 0.256 g (40%) of **3a**.

Method b. Anhydrous $CoCl_2$ (0.130 g, 1 mmol) was suspended in THF, and 2 mL of a 1 M solution of $P(CH_3)_3$ in toluene (2 mmol) was added. The color of the solution changed from deep turquoise blue to dark purple, and the mixture was further stirred for 90 min. After cooling to −78 °C, a solution of the ligand Na salt (2 mmol) in THF was filtered and added dropwise. The resulting reaction mixture was allowed to warm to room temperature and stirred for 2 h. The volatiles were evaporated in vacuum to dryness, and the residue was extracted with *n*-hexane until extracts were colorless. The resulting orange-brown solution was concentrated and cooled to −20 °C to yield 0.614 g (96%) of dark brown crystals of **3a**. Crystals suitable for X-ray diffraction were obtained.

Method c. The complex $[Co(\kappa^2N,N'\text{-}NC_4H_3C(H)=N\text{-}2,6\text{-}{}^iPr_2C_6H_3)_2]$ (**1e**) (0.283 g, 0.5 mmol) was dissolved in tetrahydrofuran (30 mL), and 2 mL of a 1 M solution of $P(CH_3)_3$ in toluene (2 mmol) were added. The initially red solution turned darker and was further stirred for 4 days at room temperature. The solvent was removed under vacuum to dryness, and the residue was extracted with *n*-hexane until extracts were colorless. The resulting solution was concentrated and stored at −20 °C to yield dark red crystals of **3a**. A second crop of crystals were obtained after partial evaporation of the mother liquor and cooling to −20 °C. Total yield: 0.100 g (31%). Attempts using shorter reaction times (e.g., 12 h, both at room temperature and 50 °C) did not afford the desired compound.

ESI-MS in CH_2Cl_2: *m/z* 640 for $[Co(L1)_2PMe_3]^+$ (L1 = $NC_4H_3C(H)=N\text{-}2,6\text{-}{}^iPr_2C_6H_3$). Anal. Found (calcd) for $C_{37}H_{51}CoN_4P$: C 69.19 (69.25), H 8.46 (8.01), N 8.65 (8.73)%.

Synthesis of $[Co(\kappa^2N,N'\text{-}NC_4H_3C(Me)=N\text{-}2,6\text{-}{}^iPr_2C_6H_3)_2(PMe_3)]$ (3b). Similar procedures described above for **3a** in methods a−c were employed (including reagent amounts), but the synthesis was carried out in diethyl ether during 36 h. The acetiminopyrrole ligand precursor was however deprotonated in a THF solution, as described for the formiminopyrrole, which was then evaporated to dryness, and the residue was redissolved in Et_2O, being further

(31) Jensen, K. A.; Nielsen, P. H.; Pedersen, C. T. *Acta Chem. Scand.* **1963**, *17*, 1115–1125.
(32) (a) Klein, H. F.; Karsch, H. H. *Chem. Ber.* **1975**, *108*, 944–955. (b) Herrman, W. A., Ed. In *Synthetic Methods of Organometallic and Inorganic Chemistry (Herrman/Brauer)*; Georg Thieme Verlag: Stuttgard, Germany, 1997; *Vol. 7*,Part 1, pp. 70−71.

Table 5. Crystal Data and Structure Refinement for Compounds **3a**, **3a·L**,[13] **4a**, **4b_I**, and **4b_II**

complex	**3a**	**3a·L**	**3b**	**4a**	**4b_I**	**4b_II**
formula	$C_{37}H_{51}CoN_4P$	$C_{54}H_{73}CoN_6P$	$C_{39}H_{55}CoN_4P$	$C_{38}H_{50}CoN_4O$	$C_{40}H_{54}CoN_4O$	$C_{40}H_{54}CoN_4O$
M	641.75	896.12	669.80	637.77	665.80	665.80
λ (Å)	0.71073	0.71073	0.71069	0.6709	0.71069	0.69040
T (K)	150	180	150	150	150	150
cryst syst	monoclinic	monoclinic	monoclinic	monoclinic	monoclinic	tetragonal
space group	$P2_1/n$	$P2_1/n$	$C2/c$	$P2_1/n$	$P2_1/c$	$I4_1/a$
a (Å)	9.31940(10)	10.9676(2)	15.9200(8)	11.6637(11)	21.665(3)	18.208(2)
b (Å)	40.7694(4)	30.2749(4)	11.1660(7)	21.386(2)	9.4940(12)	18.208(2)
c (Å)	9.90740(10)	15.4792(3)	21.0200(12)	14.1464(13)	18.167(3)	21.189(3)
α (deg)	90	90	90	90	90	90
β (deg)	110.7118(4)	92.7610(7)	101.147(3)	93.3850(10)	91.618(7)	90
γ (deg)	90	90	90	90	90	90
V (Å^3)	3521.00(6)	5133.79(15)	3666.1(4)	3522.6(6)	3735.2(9)	7024.6(17)
Z	4	4	4	4	5	4
ρ_{calcd} (g cm^{-3})	1.211	1.159	1.213	1.203	1.079	1.135
μ (mm^{-1})	0.563	0.405	0.543	0.521	0.065	0.292
θ_{max} (deg)	27	25	28	30	25.142	25.5
total data	15 157	34 727	6303	42 070	58 945	30 447
unique data	8009	9043	6303	11 528	6572	3564
R_{int}	0.019	0.140	0.034	0.028	0.047	0.119
R [$I < 3\sigma(I)$]	0.0317	0.0340	0.0597	0.0411	0.0330	0.0573
reflns R [$I < 3\sigma(I)$]	5007	3729	3649	5189	3873	1204
wR	0.0322	0.0383	0.0563	0.0441	0.0383	0.0659
GOF	1.0729	1.1287	1.1304	1.0392	1.1437	1.1394
ρ min	−0.25	−0.20	−0.97	−0.37	−0.55	−0.39
ρ max	0.23	0.38	1.36	0.38	0.59	0.67

added to the solution of $CoCl_2(PMe_3)_2$. Upon cooling of the *n*-hexane extracts of the reaction products to −20 °C, 0.586 g (87%) of dark red crystals suitable for X-ray diffraction were obtained for method a and 0.578 g (86%) of a similar material for method b. Shorter reaction times, such as 12 h, showed that reaction was not complete, and a large portion of the starting material could be recovered. Method c did not work for a reaction time up to 8 days, at 25 °C.

ESI-MS in CH_2Cl_2: m/z = 669 for $[Co(L2)_2PMe_3]^-$, (L2 = $NC_4H_3C(Me)$=N-2,6-$^iPr_2C_6H_3$). Anal. Found (calcd) for $C_{39}H_{55}CoN_4P$: C 69.74 (69.94), H 8.64 (8.28), N 8.41 (8.36)%.

Attempts to Synthesize [Co(κ²*N*,*N*′-NC$_4$H$_3$C(Me)=N-2,6-^{i}Pr$_2$C$_6$H$_3$)$_2$(PMe$_3$)] (3b) in THF. Similar procedures described above in methods a−c for the synthesis of compound **3a** in THF were employed (including reagent amounts), but using the acetiminopyrrole ligand precursor instead. However, when cooling the *n*-hexane extracts of the reaction products to −20 °C different results were obtained.

Method a. When the reaction was carried out for 2 h, 0.262 g (39%) of **3b** were obtained in the first crop and 0.367 g (55%) of the square planar **1f**[6] were obtained in the second crop. When a reaction time of 12 h was employed, 0.429 g of deep red microcrystals were obtained in the first fraction, which were showed to be a mixture of **1f** and [Co(κ²*N*,*N*′-NC$_4$H$_3$C(Me)=N-2,6-^{i}Pr$_2$C$_6$H$_3$)$_2$(OC$_4$H$_8$)] **4b.** Crystals of **4b** suitable for X-ray diffraction were obtained. The ESI-MS spectrum in THF showed two peaks at m/z 594 and 665, for $[Co(L2)_2 + H]^+$ and $[Co(L2)_2(THF)]^+$, respectively (L2 = $NC_4H_3C(Me)$=N-2,6-$^iPr_2C_6H_3$).

Method b. Complex **3b** was not obtained by this route; instead compound **1f** was obtained, in 91% yield (0.544 g). ESI-MS: m/z 594 for $[Co(L2)_2 + H]^+$.

Method c. Method c resulted in recovery of 0.468 g (78%) of the starting reagent, the square planar **1f**.

Synthesis of [Co(κ²*N*,*N*′-NC$_4$H$_3$C(H)=N-2,6-^{i}Pr$_2$C$_6$H$_3$)$_2$(OC$_4$H$_8$)] (4a). NaH (48 mg, 2 mmol) was suspended in tetrahydrofuran and 2 mmol (0.508 g) of the neutral formiminopyrrole ligand precursor was slowly added as a solid, under a counterflow of nitrogen. The resulting orange-brown solution was filtered and added dropwise to a previously cooled (−78 °C) suspension of $[Co_4Cl_8(THF)_6]$ ($CoCl_2(THF)_{1.5}$) (0.253 g, 1 mmol) in tetrahydrofuran. The mixture was stirred for an hour and then allowed to cool to room temperature. After 12 h, all volatiles were evaporated under vacuum, and the residue was extracted with *n*-hexane until extracts remained colorless. The resulting orange-brown solution was concentrated and cooled to −20 °C to yield 0.587 g (92%) of dark red crystals. Crystals suitable for X-ray diffraction were obtained.

ESI-MS in CH_2Cl_2: m/z = 637 for $[Co(L1)_2THF]^+$ (L1 = $NC_4H_3C(H)$=N-2,6-$^iPr_2C_6H_3$). Anal. Found (calcd) for $C_{38}H_{50}CoN_4O$: C 71.49 (71.56), H 7.78 (7.90), N 8.77 (8.79)%.

Synthesis of [Co(κ²*N*,*N*′-NC$_4$H$_3$C(Me)=N-2,6-^{i}Pr$_2$C$_6$H$_3$)$_2$(OC$_4$H$_8$)] (4b). A similar procedure to the described above for compound **4a** was employed (including reagent amounts), but using the acetiminopyrrole ligand precursor instead. Yield: 84% (0.560 g). Crystals suitable for X-ray diffraction were obtained.

ESI-MS in CH_2Cl_2: m/z = 665 for $[Co(L2)_2THF]^+$ (L2 = $NC_4H_3C(Me)$=N-2,6-$^iPr_2C_6H_3$). Anal. Found (calcd) for $C_{40}H_{54}CoN_4O$: C 71.87 (72.16), H 8.23 (8.17), N 8.25 (8.17)%.

Magnetic Measurements. Magnetic susceptibility measurements in solution were carried out by the Evans method[33,34] using a 3% solution of hexamethyldisiloxane (reference) in toluene-d_6.

Static DC magnetic measurements were performed on polycrystalline samples (10−20 mg) of **3a**, **b** using a multipurpose characterization system *MagLab* 2000 (Oxford Instruments) and **4a**, **b** using a *SQUID* magnetometer (Cryogenic Ltd.). The temperature dependence of the magnetization was measured under magnetic fields of 1 and 5 T in the temperature range of 1.7−300 K. The isothermal magnetization measurements up to 5 T and taken at different temperatures (1.7, 10, and 25 K) were also performed (not shown). The diamagnetism correction for the experimental data was estimated using the Pascal constants.[35]

X-ray Experimental Data. Crystallographic and experimental details of crystal structure determinations are given in Table 5. Crystals of **3a**, **3a·L**,[13] **3b**, **4a**, and **4b_I** and **4b_II** (polymorphs)

(33) Evans, D. F. *J. Chem. Soc.* **1959**, 2003–2005.
(34) Sur, S. K. *J. Magnet. Res.* **1989**, *82*, 169–173.

were isolated by filtration, and in each case, a specimen crystal selected under an inert atmosphere, covered with polyfluoroether, and mounted on the end of a nylon loop. Data for compounds **3a** and **3a·L** were collected at 150 and 180 K, respectively, on a Nonius KappaCCD with graphite-monochromated Mo Kα radiation (λ = 0.71073 Å). Crystallographic data for complex **3b** and polymorph **4b_II** were collected using graphite-monochromated Mo Kα radiation (λ = 0.71069Å) on a Bruker AXS-KAPPA APEX II diffractometer equipped with an Oxford Cryosystems open-flow nitrogen cryostat, at 150 K. Cell parameters were retrieved using Bruker[36] software and refined using Bruker SAINT[37] on all observed reflections. Absorption corrections were applied using SADABS.[38] A synchrotron radiation source was used to collect diffraction data for **4a** and polymorph **4b_I**, at 150 K. Data were collected at Station 9.8, Daresbury SRS, U.K., using a Bruker SMART CCD diffractometer. The images were processed with the DENZO and SCALEPACK programs.[39] The structures were solved by direct methods using the program SIR92.[40] The refinement (on *F*) and graphical calculations were performed for all compounds using the CRYSTALS program suite.[41] For all compounds, the non-hydrogen atoms were refined with anisotropic displacement parameters. Hydrogen atoms were located in Fourier maps and their positions adjusted geometrically (after each cycle of refinement) with isotropic thermal parameters. Chebychev weighting schemes and empirical absorption corrections were applied in each case.[42] Figures were generated using ORTEP3.[43]

Data was deposited in CCDC under the deposit numbers 652807 (**3a**), 652808 (**3a·L**), 678406 (**3b**), 678407 (**4a**), 678408 (**4b_I**), and 652809 (**4b_II**).

Computational Details. All calculations were performed with the Gaussian 03 software package,[44] using the B3LYP hybrid functional. That functional includes a mixture of Hartree−Fock[45] exchange with DFT[26] exchange-correlation, given by Becke's three parameter functional[46] with the Lee, Yang, and Parr correlation functional, which includes both local and nonlocal terms.[47,48] Geometry optimizations were performed without symmetry constraints and a basis set (b1) consisting of a standard LanL2DZ basis set[49] for Co, C, and H, with an f-polarization function added for Co,[50] while the coordinated atoms, N, O, and P were described by a standard 6−31G(d,p).[51] Spin contamination was carefully monitored for all calculations and the values of $<S^2>$ indicate minor spin contamination. The energy values referred along the text (gas phase) were obtained through single-point energy calculations using the B3LYP/b1 geometries and a 6-311G(d,p) basis set[52] (b2) for all atoms. A natural population analysis (NPA)[53] was performed with the B3LYP/b2//B3LYP/b1 density to evaluate the charge distribution on the complexes, and the Wiberg indexes obtained are used as a measure of bond strength. Spin density representations were obtained using the program Molekel 4.0.[54]

This general theoretical method has been tested before for related Co(II) complexes, yielding reasonable results.[6,9]

When mentioned in the text, solvent effects were considered in the PBE1PBE/b2//PBE1PBE/b1 energy calculations using the Polarizable Continuum Model (PCM) initially devised by Tomasi and co-workers[55] as implemented on Gaussian 03.[56] In these cases, the energy values can be taken as free energy.[57] The molecular cavity was based on the united atom topological model applied on UAHF radii, optimized for the HF/6-31G(d) level.

(35) Carlin, R. L. *Magnetochemistry*; Springer-Verlag: Berlin, 1986.
(36) *SMART Software for the CCD detector System*, version 5.625; Bruker AXS Inc.: Madison, WI, 2001.
(37) *SAINT Software for the CCD detector System*, version 7.03; Bruker AXS Inc.: Madison, WI, 2004.
(38) Sheldrick, G. M. *SADABS*, version 2.10; Bruker AXS Inc.: Madison, WI, 2003.
(39) Otwinowski, Z.; Minor, W. in Eds. Carter, C. N., Jr.; Sweet, R. M. In *Methods Enzymology*; Academic Press: New York, 1996; p 276.
(40) For SIR92, see: Altomare, A.; Cascarano, G. L.; Giacovazzo, C.; Guagliardi, A. *J. Appl. Crystallogr.* **1993**, *26*, 343–350.
(41) (a) Watkin, D. J.; Prout, C. K.; Carruthers, J. R.; Betteridge, P. W. *CRYSTALS*: Oxford U.K., 1996. (b) Betteridge, P. W.; Carruthers, J. R.; Cooper, R. I.; Prout, K.; Watkin, D. J. *J. Appl. Crystallogr.* **2003**, *36*, 1487. (c) Watkin, D. J.; Prout, C. K.; Pearce, L. J. *CAMERON*; Oxford U.K., 1996.
(42) Walker, N.; Stuart, D. *Acta Crystallogr., Sect. A* **1983**, *39*, 158–166.
(43) For ORTEP3 for Windows, see: Farrugia, L. J. *J. Appl. Crystallogr.* **1997**, *30*, 565–566.
(44) Frisch, M. J.; Trucks, G. W.; Schlegel, H. B.; Scuseria, G. E.; Robb, M. A.; Cheeseman, J. R.; Montgomery, J. A., Jr.; Vreven, T.; Kudin, K. N.; Burant, J. C.; Millam, J. M.; Iyengar, S. S.; Tomasi, J.; Barone, V.; Mennucci, B.; Cossi, M.; Scalmani, G.; Rega, N.; Petersson, G. A.; Nakatsuji, H.; Hada, M.; Ehara, M.; Toyota, K.; Fukuda, R.; Hasegawa, J.; Ishida, M.; Nakajima, T.; Honda, Y.; Kitao, O.; Nakai, H.; Klene, M.; Li, X.; Knox, J. E.; Hratchian, H. P.; Cross, J. B.; Bakken, V.; Adamo, C.; Jaramillo, J.; Gomperts, R.; Stratmann, R. E.; Yazyev, O.; Austin, A. J.; Cammi, R.; Pomelli, C.; Ochterski, J. W.; Ayala, P. Y.; Morokuma, K.; Voth, G. A.; Salvador, P.; Dannenberg, J. J.; Zakrzewski, V. G.; Dapprich, S.; Daniels, A. D.; Strain, M. C.; Farkas, O.; Malick, D. K.; Rabuck, A. D.; Raghavachari, K.; Foresman, J. B.; Ortiz, J. V.; Cui, Q.; Baboul, A. G.; Clifford, S.; Cioslowski, J.; Stefanov, B. B.; Liu, G.; Liashenko, A.; Piskorz, P.; Komaromi, I.; Martin, R. L.; Fox, D. J.; Keith, T.; Al-Laham, M. A.; Peng, C. Y.; Nanayakkara, A.; Challacombe, M.; Gill, P. M. W.; Johnson, B.; Chen, W.; Wong, M. W.; Gonzalez, C.; Pople, J. A. *Gaussian 03*, revision C.02; Gaussian, Inc.: Wallingford, CT, 2004.
(45) Hehre, W. J.; Radom, L.; Schleyer P. v. R.; Pople, J. A. *Ab Initio Molecular Orbital Theory*; John Wiley & Sons: New York, 1986.
(46) Becke, A. D. *J. Chem. Phys.* **1993**, *98*, 5648–5652.
(47) Lee, C.; Yang, W.; Parr, R. G. *Phys. Rev. B.* **1988**, *37*, 785–789.
(48) Miehlich, B.; Savin, A.; Stoll, H.; Preuss, H. *Chem. Phys. Lett.* **1989**, *157*, 200–206.
(49) (a) Dunning, T. H., Jr.; Hay, P. J. *Modern Theoretical Chemistry*; Schaefer, H. F., III, Ed.; Plenum: New York, 1976, *Vol. 3*, p 1. (b) Hay, P. J.; Wadt, W. R. *J. Chem. Phys.* **1985**, *82*, 270–283. (c) Wadt, W. R.; Hay, P. J. *J. Chem. Phys.* **1985**, *82*, 284–298. (d) Hay, P. J.; Wadt, W. R. *J. Chem. Phys.* **1985**, *82*, 299–310.
(50) Ehlers, A. W.; Böhme, M.; Dapprich, S.; Gobbi, A.; Höllwarth, A.; Jonas, V.; Köhler, K. F.; Stegmann, R.; Veldkamp, A.; Frenking, G. *Chem. Phys. Lett.* **1993**, *208*, 111–114.
(51) (a) Ditchfield, R.; Hehre, W. J.; Pople, J. A. *J. Chem. Phys.* **1971**, *54*, 724–728. (b) Hehre, W. J.; Ditchfield, R.; Pople, J. A. *J. Chem. Phys.* **1972**, *56*, 2257–2261. (c) Hariharan, P. C.; Pople, J. A. *Mol. Phys.* **1974**, *27*, 209–214. (d) Gordon, M. S. *Chem. Phys. Lett.* **1980**, *76*, 163–168. (e) Hariharan, P. C.; Pople, J. A. *Theor. Chim. Acta* **1973**, *28*, 213–222.
(52) (a) McClean, A. D.; Chandler, G. S. J. *Chem. Phys.* **1980**, *72*, 5639–5648. (b) Krishnan, R.; Binkley, J. S.; Seeger, R.; Pople, J. A. *J. Chem. Phys.* **1980**, *72*, 650–654. (c) Wachters, A. J. H. *J. Chem. Phys.* **1970**, *52*, 1033–1036. (d) Hay, P. J. *J. Chem. Phys.* **1977**, *66*, 4377–4384. (e) Raghavachari, K.; Trucks, G. W. *J. Chem. Phys.* **1989**, *91*, 1062–1065. (f) Binning, R. C.; Curtiss, L. A. *J. Comput. Chem.* **1995**, *103*, 6104–6113. (g) McGrath, M. P.; Radom, L. *J. Chem. Phys.* **1991**, *94*, 511–516.
(53) (a) Carpenter, J. E.; Weinhold, F. *J. Mol. Struct.—Theochem* **1988**, *169*, 41–62. (b) Carpenter, J. E. *PhD Thesis*, University of Wisconsin, Madison, WI, 1987. (c) Foster, J. P.; Weinhold, F. *J. Am. Chem. Soc.* **1980**, *102*, 7211–7118. (d) Reed, A. E.; Weinhold, F. *J. Chem. Phys.* **1983**, *78*, 4066–4073. (e) Reed, A. E.; Weinhold, F. *J. Chem. Phys.* **1985**, *78*, 1736–1740. (f) Reed, A. E.; Weinstock, R. B.; Weinhold, F. *J. Chem. Phys.* **1985**, *83*, 735–746. (g) Reed, A. E.; Curtiss, L. A.; Weinhold, F. *Chem. Rev.* **1988**, *88*, 899–926. (h) Weinhold, F.; Carpenter, J. E. In *The Structure of Small Molecules and Ions*; Plenum: New York, 1988; p 227.
(54) Flükiger, P.; Lüthi, H. P.; Portmann, S.; Weber, J. Swiss Center for Scientific Computing, Manno, Switzerland, 2000.
(55) (a) Cancès, M. T.; Mennucci, B.; Tomasi, J. J. *Chem. Phys.* **1997**, *107*, 3032. (b) Cossi, M.; Barone, V.; Mennucci, B.; Tomasi, J. *Chem. Phys. Lett.* **1998**, *286*, 253. (c) Mennucci, B.; Tomasi, J. J. *Chem. Phys.* **1997**, *106*, 5151.
(56) Tomasi, J.; Mennucci, B.; Cammi, R. *Chem. Rev.* **2005**, *105*, 2999.
(57) Cossi, M.; Scalmani, G.; Rega, N.; Barone, V. J. *Chem. Phys.* **2002**, *117*, 43.

Acknowledgment. We thank the Fundação para a Ciência e Tecnologia for financial support (Project POCI/QUI/59025/2004, cofinanced by FEDER) and for fellowships to S.A.C. (SFRH/BPD/14902/2004 and SFRH/BPD/34974/2007) and R.M.B. (SFRH/BPD/3574/2000), respectively. We also thank the Royal Society for funding to S.I.P. Thanks are also due to Dr. Joaquim Marçalo, ITN, Sacavém, Portugal, for the calculation of cone angles (equivalent) of PMe_3 and THF and for helpful discussions.

Supporting Information Available: CIF files containing X-ray structural data, including data collection parameters, positional and thermal parameters, and bond distances and angles, for all compounds of this work, table containing selected bond distances and angles for all crystal structures of this work (Table S1), figures containing the definition of parameter τ (Figure S1), the X-ray structures of compounds **3a·L** and **4b** (polymorph **4b_II**) (Figures S2−S4), the Curie−Weiss plots of the magnetic susceptibility data of compounds **3a**,**b** and **4a**,**b** (Figures S5 and S6), views of the crystal packings of complexes **4a** and **4b_I** (Figures S7 and S8), the optimized geometries and relative energy difference of the high-spin and low-spin ground states of complexes **3a** and **3b** (Figure S9) and **4a** and **4b** (Figure S10), and the spin density for the low-spin isomers of complexes **3a** and **4a** (Figure S11) and **3b** and **4b** (Figure S12), and tables of atomic coordinates for all optimized species (Table S2).This material is available free of charge via the Internet at http://pubs.acs.org.

IC800992F